

Review

CO₂ Recycling to Dimethyl Ether: State-of-the-Art and Perspectives

Enrico Catizzone ^{1,*} , Giuseppe Bonura ² , Massimo Migliori ¹, Francesco Frusteri ² and Girolamo Giordano ¹

¹ Department of Environmental and Chemical Engineering, University of Calabria, Via P. Bucci, 87036 Rende (CS), Italy; massimo.migliori@unical.it (M.M.); ggiordanaunical@yahoo.it (G.G.)

² CNR-ITAE “Nicola Giordano”, Via S. Lucia Sopra Contesse 5, 98126 Messina, Italy; giuseppe.bonura@itae.cnr.it (G.B.); francesco.frusteri@itae.cnr.it (F.F.)

* Correspondence: enrico.catizzone@unical.it; Tel.: +39-098-449-6669

Received: 13 November 2017; Accepted: 22 December 2017; Published: 24 December 2017

Abstract: This review reports recent achievements in dimethyl ether (DME) synthesis via CO₂ hydrogenation. This gas-phase process could be considered as a promising alternative for carbon dioxide recycling toward a (bio)fuel as DME. In this view, the production of DME from catalytic hydrogenation of CO₂ appears as a technology able to face also the ever-increasing demand for alternative, environmentally-friendly fuels and energy carriers. Basic considerations on thermodynamic aspects controlling DME production from CO₂ are presented along with a survey of the most innovative catalytic systems developed in this field. During the last years, special attention has been paid to the role of zeolite-based catalysts, either in the methanol-to-DME dehydration step or in the one-pot CO₂-to-DME hydrogenation. Overall, the productivity of DME was shown to be dependent on several catalyst features, related not only to the metal-oxide phase—responsible for CO₂ activation/hydrogenation—but also to specific properties of the zeolites (i.e., topology, porosity, specific surface area, acidity, interaction with active metals, distributions of metal particles, ...) influencing activity and stability of hybridized bifunctional heterogeneous catalysts. All these aspects are discussed in details, summarizing recent achievements in this research field.

Keywords: CO₂ hydrogenation; dimethyl ether; low-carbon processes; thermodynamics; catalysis; zeolites

1. Introduction: How Can CO₂ Become the Future Carbon Source?

Carbon dioxide is recognized as the main responsible of the super green-house effect, causing global warming and climate change. In this concern, to avoid more dangerous consequences, the Intergovernmental Panel on Climate Change (IPCC) and the United Nations Climate Change Conference (COP21, Paris, 2015) have emphasized the need to reduce CO₂ emissions by at least one half of the current value by 2050, aiming at limiting the global average temperature increase to a maximum of 2 °C [1]. Carbon dioxide is mainly emitted from power plants (e.g., coal-based) and vehicles, but also other industrial sources contribute to increase the CO₂ emission into the atmosphere, such as boilers or cement and steel plants [2]. The growing world population, the enhancement of welfare, the change in food habits are also causing an increase of animal farms so boosting CO₂ emissions [3]. Aiming at reducing CO₂ emissions, a carbon tax has been proposed from several countries as a strategy able to balance the incremental costs of reducing carbon emissions with the incremental benefits for limiting damages due to climate changes causing additional costs for industry [4].

During the last decades, several strategies and technologies have been developed concerning capture and storage of carbon dioxide (CCS) and, by 2020, the number of projects dealing with this

topic is expected to double even if few large-scale CCS plants are already working [2]. On the other hand, during the last years, the scientific community started to consider CO₂ not as an expensive waste (especially in the countries where carbon taxes are applied) but mainly as potential carbon source, alternative to the fossil-ones. Therefore, the future perspectives of carbon dioxide emissions reduction will not only concern the development of more efficient CCS technologies but will involve new strategies development for CO₂ recycling to energy vectors and chemical intermediates. In this concern, the conversion of CO₂ to dimethyl ether (DME) has received renewed attention since DME can be used as an intermediate to produce several value-added products (gasoline, aromatics and olefin) or as an alternative fuel as detailed below [5].

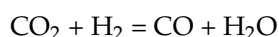
DME, the simplest of the ethers, is a neither toxic nor carcinogenic molecule with a boiling point of −25 °C, but it is a liquid at room temperature under a relatively low pressure (≈0.5 MPa) [6]. Chemical and physical properties of DME are close to liquid petroleum gas (LPG) and published studies suggested that the technologies developed for storage and transport of LPG can be easily converted to accommodate DME with similar safety guidelines and codes [7]. DME is also an important chemical intermediate for production of widely used chemicals, such as diethyl sulphate, methyl acetate and, as mentioned before, light olefins and gasoline [8]. Nowadays, DME is mainly used as aerosol propellant in spray cans, replacing the banned ozone-destroying chlorofluorocarbon (CFC) compounds but, in the last decades, it is receiving a growing attention also as alternative and eco-friendly fuel. In 1995, an extensive collaborative research effort by Amoco (currently BP), Haldor Topsøe and Navistar International Corporation, demonstrated that DME could be a reliable alternative fuel for diesel engines with low-emission of NO_x, SO_x and particulate, to be produced at large-scale from methanol through a dehydration step [9]. These studies renewed attention on the outstanding performances of DME as alternative fuel to diesel and showed total compliance with the hardly strict California ultra-low emission vehicle (ULEV) regulations for medium-duty vehicles. Because of the large scale changes in fuel infrastructure, the global implementation of DME to power vehicles still remains an open challenge. Indeed, the primary DME market was the blending of DME with LPG and Amoco patented a DME/LPG blend for automotive applications [10], while the other future market perspectives of use of DME as fuel are: (1) alternative fuel for diesel engines; (2) fuel for power generation in gas turbine plants; (3) chemical intermediate for olefins and synthetic gasoline production. Therefore, rather than methanol, dimethyl ether can be considered both as reliable energy vector of the future and as chemical intermediate in low-carbon processes. In this concern, carbon dioxide can be used as reactant to produce methanol and then DME. Specifically, methanol is first produced from the hydrogenation of carbon dioxide, according to the following reaction:



Then, DME is formed via alcohol dehydration:



By considering the reverse water shift reaction:



The global reaction leading to the formation of DME is:



As stoichiometry suggests, six moles of hydrogen are necessary per mole of DME and there are no real advantages to adopt this pathway to produce DME (or even methanol) via CO₂ hydrogenation, since hydrogen is usually produced from fossil hydrocarbons (mainly from natural gas or light hydrocarbons). Therefore, only if hydrogen is produced from non-fossil sources, the Methanol/DME

Economy Theory will be a reliable option; in particular, if hydrogen is directly produced using renewable energy sources, carbon dioxide hydrogenation will become a valuable strategy for renewable energy utilization in both chemical industry and power generation. Hydrogen can be produced from renewables in several ways. The current approach is the production of electrical energy by using renewable energy sources (e.g., solar energy) and the use of this energy for water electrolysis using Fuel Cells [11]. Other approaches to hydrogen production were also investigated: hydrogen from cyanobacteria or algae [12,13], biomass thermo-chemical process or anaerobic fermentation [14,15] or water splitting via photo-electrolysis [16,17].

Although hydrogen production from renewables remains an open challenge, the carbon-cycle based on CO₂ Hydrogenation can be summarized in five steps (Figure 1):

- Production of hydrogen via water splitting by using renewable energy (e.g., solar energy);
- Capture and safe storage of CO₂ from power plants emission or even from atmosphere;
- Hydrogenation of captured CO₂ to produce methanol and/or DME (DME should be preferred because of its no-toxicity);
- Utilization of DME for energy production or as intermediate in the chemical-chain industry;
- Reuse the carbon dioxide from eco-friendly combustion of DME to re-produce itself.

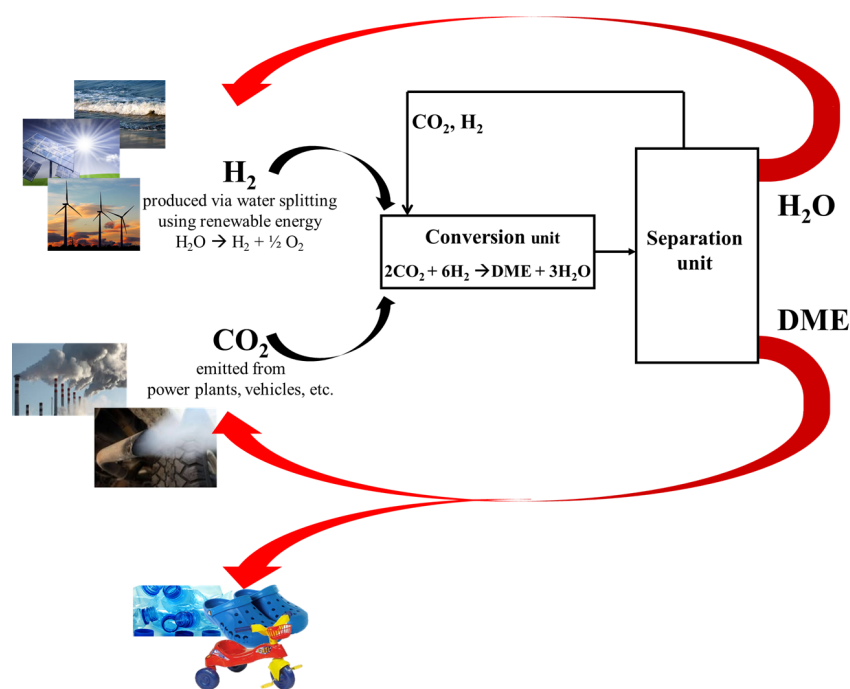


Figure 1. Proposed carbon cycle loop involving CO₂ as energy vector.

Following this strategy and increasing the research on the listed steps, it will be possible to create an efficient CO₂-based production system for both chemicals and energy production, compromising between energy request (also reducing the dependence on fossil sources) and socio-environmental safety (lowering the carbon dioxide emission into the atmosphere) [11]. Among the several challenges still open, despite several works have been carried out during the last years, the development of a highly efficient catalyst for CO₂ hydrogenation is still a stimulating challenge. Since the formation of DME via one-pot CO₂ hydrogenation involves two reaction steps (methanol formation and dehydration), the catalyst should exhibit a redox function able to hydrogenate CO₂ to alcohol and an acid function able to convert the alcohol in the ether. Several strategies have been proposed in order to create a catalyst able to produce DME via one-pot hydrogenation of CO₂ with good performances in

terms of CO₂ conversion, DME selectivity and stability. Recently, Álvarez et al. [18] discussed some catalytic aspects concerning one-pot CO₂-to-DME process, revealing that further advances in research are necessary to reach high catalytic activity. In fact, despite Cu-based catalyst is expected to remain the most efficient catalyst for CO₂-to-methanol reaction step, some aspects about bifunctional catalyst such as: (i) the choice of the acid function, (ii) the method used to prepare hybrid catalyst, (iii) the copper particle sintering and (iv) the catalyst deactivation, remain the main open issues in view of an optimization of the process.

After a brief discussion about the use of DME as alternative fuel and thermodynamics of CO₂-to-DME process, this paper focus on the critical evaluation of proposed catalytic systems, paying particular attention to the effects of both physicochemical properties on redox/acid functions and preparation method on catalytic performance of hybrid catalyst, emphasizing on the potential of zeolites as efficient acid catalysts for methanol dehydration step.

2. DME as Valuable Fuel of the Future

Since the middle of 1990s DME has been identified as a reliable diesel alternative for auto transportation. A chemical-physical property comparison between diesel fuel and DME is reported in Table 1, allowing one to identify both the advantages and disadvantages of using DME as an alternative fuel in such engines. A lower boiling point leads to a faster evaporation when liquid DME is injected into the engine cylinder, improving the combustion. In addition, a lower auto-ignition temperature allows one to obtain a higher cetane number for DME than that exhibited by diesel fuel. Generally, a high cetane number results in easy ignition, more complete combustion and cleaner exhaust gases; in addition, a high cetane number allows one to reduce not only noise but also fuel consumption and exhaust gas emissions during engine warm-up [6,19]. In addition, based on the similar chemical-physical properties between DME and LPG, existing infrastructure as the storage vessels and fuel lines used in LPG-based systems can also be used for DME.

Table 1. Physicochemical properties of DME and diesel fuels [6].

Property	Unit	DME	Diesel
Carbon content	mass%	52.2	86
Hydrogen content	mass%	1–3	14
Oxygen content	mass%	34.8	0
Carbon-to-hydrogen ratio	-	0.337	0.516
Liquid density	kg/m ³	667	831
Cetane number	-	>55	40–50
Autoignition temperature	K	508	523
Stoichiometric air/fuel mass ratio	-	9.6	14.6
Normal boiling point	K	248.1	450–643
Enthalpy of vaporization	kJ/kg	467.1	300
Lower heating value	MJ/kg	27.6	42.5
Ignition limits	vol% in air	3.4/18.6	0.6/6.5
Elastic Modulus	N/m ²	6.37 × 10 ⁸	14.86 × 10 ⁸
Liquid kinematic viscosity	cSt	<0.1	3
Surface tension (at 298 K)	N/m	0.012	0.027
Vapour pressure (at 298 K)	kPa	530	<10

On the other hand, some disadvantages should also be taken into account to complete the evaluation of DME as substitute of diesel: DME exhibits a much lower LHV than diesel fuel (27.6 MJ/kg vs. 42.5 MJ/kg) and, for this reason, a larger amount of injected volume and longer injection period for DME is necessary in order to deliver the same amount of energy. Other disadvantages are related to the necessity to change the engine configuration if diesel fuel is substituted with DME. In fact, the lower viscosity of DME requires special gaskets to prevent fuel leakage. In addition, DME can act as a solvent for some organic compounds causing incompatibility with elastomers and plastic materials. Therefore, a careful selection of materials is required when DME is used as fuel in diesel engines [20].

The diesel-fueled compression ignition (CI) engine offers several advantages compared to a gasoline-fueled spark ignition (SI) engine (e.g., better fuel economy, higher power performance, and longer expected life).

Nevertheless, CI engines have several well-known drawbacks because of the higher temperature in the combustion chamber and the physical-chemical characteristics of diesel fuel, so that harmful pollutants are emitted, such as nitrogen oxides (NO_x), particulate (PM), hydrocarbon compounds (HC), carbon monoxide (CO) and sulphur oxides (SO_x). As reported by Park et al. [20], emissions of HC and CO are lower if DME is burned in a CI engine, whilst the absence of sulphur in DME fuel allows one to obtain SO_x-free exhaust gases. Aiming to reduce the formation of particulate (soot), typical of diesel-fed CI engines, an anti-particulate filter (APF) should be used. The high oxygen content and the absence of C-C bonds in DME molecule does not favour formation of soot during combustion, eliminating the already described problem associated with diesel fuel. Experimental results reported by Sidhu et al. [21] showed that the relative particulate yield from DME was just 0.026% versus the value of 0.51% exhibited by both diesel and bio-diesel fuels. For this reason, an APF is not required in DME-fueled engines. Thanks to this advantage, the installation and application of oxidation catalysts for further reduction of both HC and CO is possible in terms of economy and vehicle space.

A trustworthy experimental comparison of NO_x emissions from CI engines when using DME or diesel fuel is not easy to perform because the results strongly depend on the engine conditions and the fuel supply system. Usually, a higher NO_x level was detected when diesel fuels were substituted with DME, as reported by Park et al. [20] and Kim et al. [22], but opposite results have been published in SAE International studies [23,24]. Unlike diesel fuel, the reduced emissions of the other pollutants allows one to use high exhaust gas recirculation (EGR), thus decreasing the NO_x level without any increase in PM and soot emissions [19].

On the other hand, not only the combustion performance has to be taken into account when assessing the possibility of using a substance as an alternative fuel. In fact, a careful evaluation of the efficiency of each step, from the raw material supply to utilization of the final fuel is required. In this concern, a well-to-wheels (WTW) analysis is usually performed. A well-to-wheels analysis consists of a well-to-tank (WTT) and a tank-to wheels (TTW) analysis [19]. The WTT analysis can be carried out by calculating the WTT efficiency as the ratio between the energy of the fuel (e.g., in terms of lower heat value, LHV) and the sum of energy consumptions in each manufacturing step, from feedstock recovery to fuel distribution. Among the alternative fuels derived from natural gas, biomass or electrolysis (e.g., DME, methanol, synthetic diesel, hydrogen, etc.), DME exhibits the highest WTT efficiency [19]. TTW analysis includes everything related to the vehicle and its characteristics and for these reasons different fuels have to be compared under the same engine technology and, in this context, DME exhibits high engine efficiency for several vehicle technologies. By coupling WTT and TTW analysis, in order to estimate a WTW efficiency, Semelsberg et al. [19] according to Arcoumanis et al. [6], suggest that DME ranks on the top among different alternative fuels for several vehicle technologies. The WTW efficiency of DME is comparable with LPG and compressed natural gas (CNG)-fueled vehicles, but lower than vehicles operating with diesel fuel.

Because of the clean emission offered during its combustion, DME is also suggested as fuel for power generation by using gas turbines. In the last decade, several companies (including BP, Snamprogetti/ENI S.p.A, Haldor Topsøe) [25] have tested DME as a gas turbine fuel in the case of reduced natural gas availability. As mentioned above, the physico-chemical properties of DME are close to those of LPG, which allows ocean transport using conventional LPG tankers without any additional effort. Several studies have demonstrated that DME is a clean fuel alternative to natural gas, in terms of both NO_x and CO emissions [26,27]. Depending on the operation conditions, DME can emit more CO than NO_x [28], but this disadvantage can be overcome by a slight nozzle modification [29].

As already discussed, hydrogen generation remains the major issue to boost the proposed CO₂-based scenario, involving DME as energy vector [30,31]. Production of hydrogen by steam reforming of methane or gasoline is the main industrial process to produce hydrogen and these

processes require high temperatures (above 600 °C for methane and above 800 °C for gasoline), high energy demand, stable catalysts and expensive insulated reactors. Recently, steam reforming of methanol is receiving attention because of the relative low process temperature (around 300 °C) and simpler reactor configurations [32]. Nevertheless, due to the high toxicity of methanol, DME is also considered a reliable candidate for hydrogen production by steam reforming (by adopting similar operation conditions of methanol steam reforming and over a bifunctional catalyst, namely an acid function for DME hydrolysis to methanol and a copper-based catalyst for the alcohol reforming), being not toxic and with a high hydrogen content [33–36].

3. Thermodynamic Considerations on CO₂-to-DME Process

CO₂ hydrogenation to DME usually involves four reactions summarized in Table 2.

Table 2. List of reactions involved in one-pot CO₂ hydrogenation to DME.

Reaction No.	Reaction Stoichiometry	$\Delta\tilde{H}^{\circ}_{298K}$
1	CO ₂ + 3H ₂ = CH ₃ OH + H ₂ O	−49.5 kJ/mol _{CO₂}
2	2CH ₃ OH = CH ₃ OCH ₃ + H ₂ O	−23.4 kJ/mol _{DME}
3	CO ₂ + H ₂ = CO + H ₂ O	+41.2 kJ/mol _{CO₂}
4	CO + 2H ₂ = CH ₃ OH	−90.6 kJ/mol _{CO}

For all of the involved reactions it is possible to calculate the equilibrium constants, as follows:

$$K_j(T) = \prod_i a_i^{v_{ij}} = \exp\left(\frac{-\Delta\tilde{G}_{rj}}{RT}\right) \quad (1)$$

where a_i is the activity of the specie i involved in the reaction j with the stoichiometric number v_{ij} , while $\Delta\tilde{G}_{rj}$ is the molar Gibbs energy change of the reaction j that can be calculated from the following equation:

$$\Delta\tilde{G}_{rj} = \sum_i v_{ij} \tilde{G}_i(T, P) \quad (2)$$

Since all species are in gaseous phase a state standard activity of pure gas at 1 bar can be chosen as reference to compute activity:

$$a_i = \frac{\bar{f}_i}{1 \text{ bar}} \quad (3)$$

where \bar{f}_i is the fugacity of the specie i in the gaseous mixture that has been computed adopting Peng-Robinson equation of state for the mixture.

Therefore, the equilibrium constants can be expressed as follows:

$$K_1(T) = \frac{\bar{f}_{\text{CH}_3\text{OH}} \cdot \bar{f}_{\text{H}_2\text{O}}}{\bar{f}_{\text{CO}_2} \cdot \bar{f}_{\text{H}_2}^2} = \exp\left(\frac{-\Delta\tilde{G}_{r1}^0(T)}{RT}\right) \quad (4)$$

$$K_2(T) = \frac{\bar{f}_{\text{CH}_3\text{OCH}_3} \cdot \bar{f}_{\text{H}_2\text{O}}}{\bar{f}_{\text{CH}_3\text{OH}}^2} = \exp\left(\frac{-\Delta\tilde{G}_{r2}^0(T)}{RT}\right) \quad (5)$$

$$K_3(T) = \frac{\bar{f}_{\text{CO}} \cdot \bar{f}_{\text{H}_2\text{O}}}{\bar{f}_{\text{CO}_2} \cdot \bar{f}_{\text{H}_2}} = \exp\left(\frac{-\Delta\tilde{G}_{r3}^0(T)}{RT}\right) \quad (6)$$

$$K_4(T) = \frac{\bar{f}_{\text{CH}_3\text{OCH}_3}}{\bar{f}_{\text{CO}_2} \cdot \bar{f}_{\text{H}_2}^2} = \exp\left(\frac{-\Delta\tilde{G}_{r4}^0(T)}{RT}\right) \quad (7)$$

Then, the mass balance on the specie i can be written as:

$$n_i^{eq} = n_i^0 + \sum_j v_{ij} \zeta_j \quad (8)$$

where n_i^{eq} and n_i^0 are the final and the initial moles of the specie i , while ζ_j is the extent of the reaction j .

Accordingly, the CO₂ equilibrium conversion can be calculated as follows:

$$X_{CO_2} = \frac{n_{CO_2}^0 - n_{CO_2}^{eq}}{n_{CO_2}^0} = \frac{\zeta_1 + \zeta_3}{n_{CO_2}^0} \quad (9)$$

Whilst selectivity towards DME, MeOH and CO, on C-basis, are defined according to the following equations:

$$S_{DME} = \frac{2 \cdot \zeta_2}{\zeta_1 + \zeta_3} \quad (10)$$

$$S_{MeOH} = \frac{\zeta_1 + \zeta_4 - \zeta_2}{\zeta_1 + \zeta_3} \quad (11)$$

$$S_{CO} = \frac{\zeta_3 - \zeta_4}{\zeta_1 + \zeta_3} \quad (12)$$

In this paragraph, the effect of reaction parameters, such as reaction temperature, reaction pressure and inlet H₂/CO₂ ratio, on thermodynamics of one-pot CO₂ hydrogenation to DME are discussed. Simulation was performed using Unisim Design R430 software (Honeywell, Morristown, NJ, USA), by assuming only CO₂ and H₂ in the reactant mixture.

Figure 2 reports the equilibrium theoretical conversion of CO₂ as a function of reaction temperature and pressure, calculated for an initial H₂/CO₂ molar ratio equal to 3.

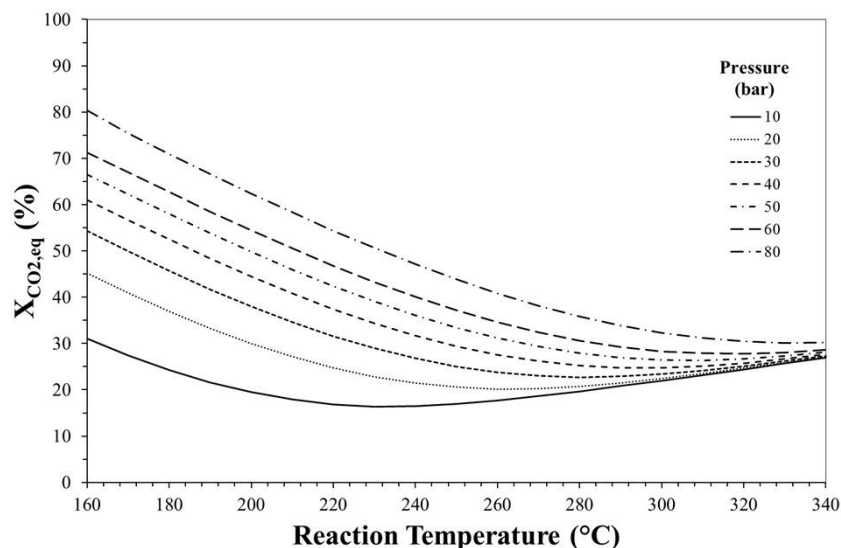


Figure 2. Effect of reaction temperature and pressure on CO₂ equilibrium conversion. H₂/CO₂ (mol/mol) = 3.

The increase in reaction pressure promotes CO₂ conversion since global reaction proceeds with a decrease in the number of moles even if this effect becomes less evident at high temperature. On the contrary, since the process involves both exothermic (i.e., step 1, 2 and 4 of Table 2) and endothermic (i.e., step 3) reactions, the effect of increase in temperature on CO₂ equilibrium conversion is disadvantageous at low temperature and advantageous at high temperature, even if this effect is

more marked at low pressure. For instance, at 10 bar, $X_{\text{CO}_2,\text{eq}}$ decreases from ca. 30% to ca. 16% when the temperature increases from 160 °C to 230 °C and it increases to ca. 28% if the reaction temperature rises to 340 °C, suggesting that at high temperature the reverse water gas shift reaction (that also favours CO_2 consumption) predominates over the other steps.

Figures 3–5 show the effects of reaction temperature and pressure on selectivity towards DME, CO and methanol, respectively. As mentioned before, low temperature should be adopted for favouring exothermic reactions and achieving high DME selectivity. In fact, high temperatures favour rWGS promoting CO formation and lowering selectivity towards DME.

Especially at high temperature, DME selectivity can be improved by increasing the reaction pressure. For instance, at 240 °C, DME equilibrium selectivity can be increased from ca. 20% to ca. 60% by pressuring the system from 10 bar to 30 bar, while selectivity towards CO can be reduced from ca. 70% to values below 20%.

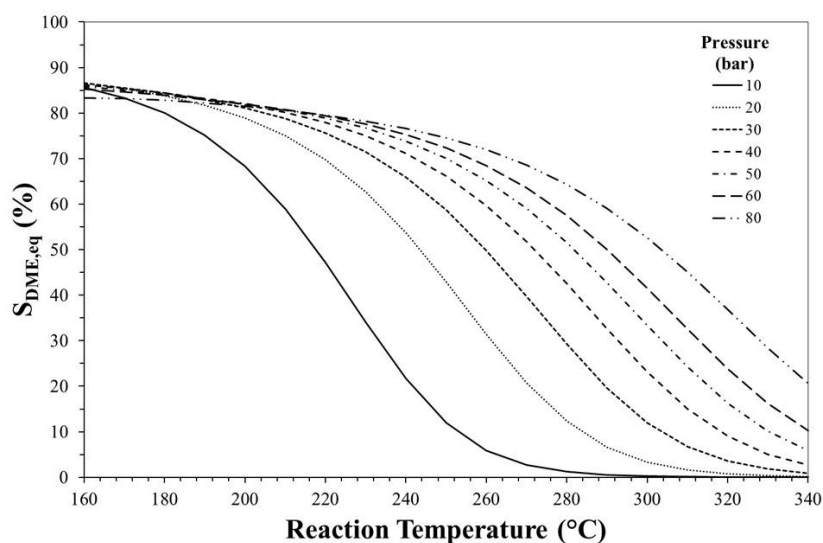


Figure 3. Effect of reaction temperature and pressure on DME equilibrium selectivity. Initial H_2/CO_2 molar ratio equals to 3.

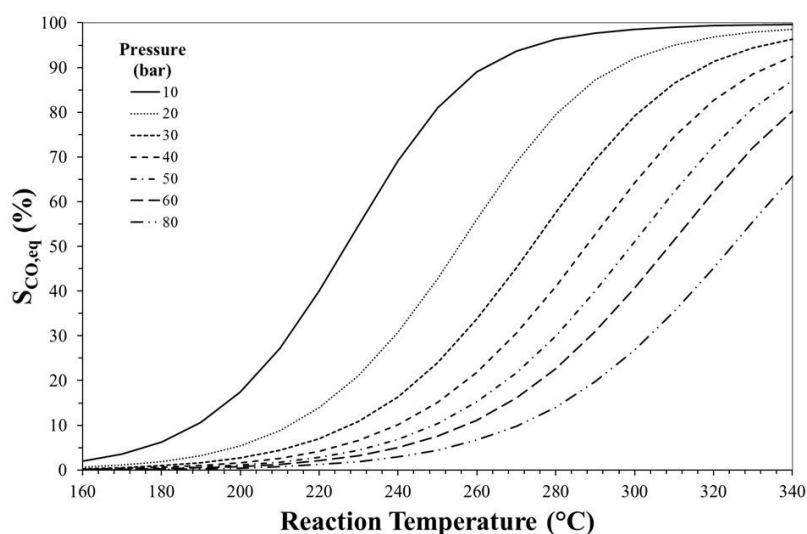


Figure 4. Effect of reaction temperature and pressure on CO equilibrium selectivity. Initial H_2/CO_2 molar ratio equals to 3.

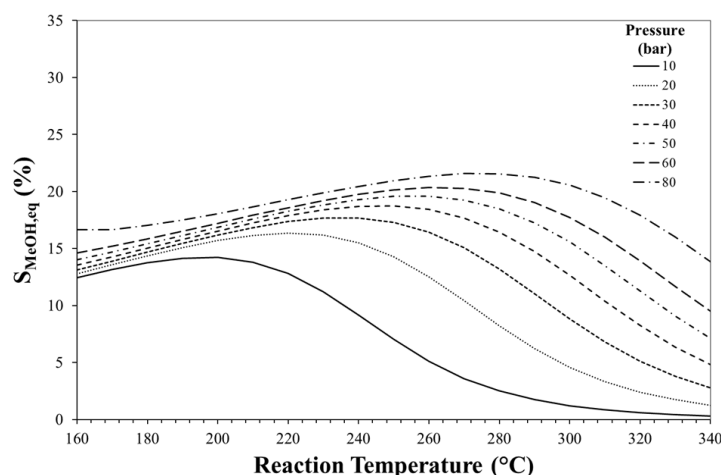


Figure 5. Effect of reaction temperature and pressure on methanol equilibrium selectivity. Initial H_2/CO_2 molar ratio equal to 3.

The equilibrium selectivity towards methanol is favoured by high pressure and low temperature even if it can be estimated always lower than 20%. Also the reactant mixture composition strongly affects process thermodynamics as shown in Figure 6.

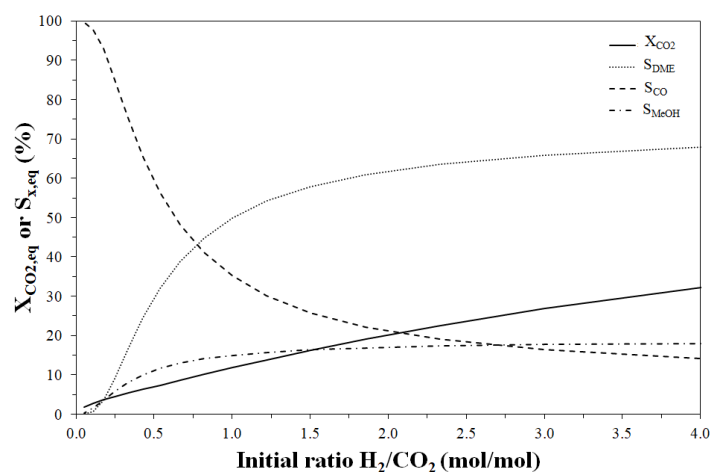


Figure 6. Effect of initial H_2/CO_2 molar ratio on CO_2 equilibrium conversion and DME, CO and methanol equilibrium selectivity. Reaction temperature and pressure: 240 °C and 30 bar, respectively.

Increasing the H_2/CO_2 molar ratio in the feedstock, the CO_2 conversion also increases and a H_2/CO_2 value higher than 0.8 mol $_{H_2}$ /mol $_{CO_2}$ (at 240 °C and 30 bar) should be adopted in order to obtain a selectivity to DME higher than that to CO. In fact, a higher CO_2 concentration favours CO formation from rWGS causing a DME selectivity loss. On the contrary, higher DME selectivity values can be predicted for a higher H_2 initial content, even if the effect is much more pronounced at low H_2/CO_2 ratio.

The Effect of Methanol Dehydration Reaction Step on Thermodynamics

It is well known that DME production from CO_2 can be carried out in a two-step process in which methanol is produced via CO_2 hydrogenation in a first reactor, purified and then dehydrated to produce DME in another reactor, whilst in “one-pot” process both reaction steps are simultaneously

carried out in the same reactor [37]. Figure 7 shows the effect of temperature and pressure on CO₂ conversion for both one-step and two-step process.

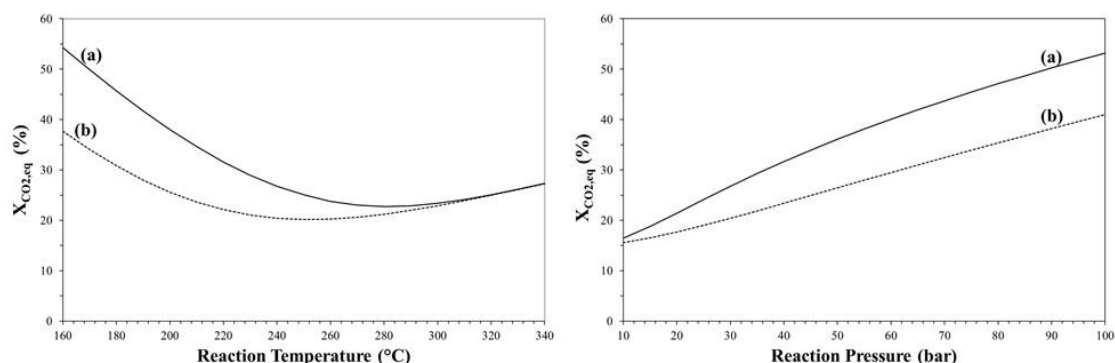


Figure 7. CO₂ equilibrium conversion of CO₂-to-DME (a) and CO₂-to-MeOH (b) process as a function of reaction temperature (left) and pressure (right).

Due to methanol consumption by dehydration reaction (2), the one-step process is more efficient than the two-step process in terms of CO₂ equilibrium, even if such a thermodynamic benefit is more valuable at low temperature and high pressure.

In order to quantify the thermodynamic benefit of using the one-pot process, the CO₂ conversion gain (CPG) can be calculated as follows:

$$CPG = \frac{X_{CO_2,eq}^a - X_{CO_2,eq}^b}{X_{CO_2,eq}^b} \cdot 100 \quad (13)$$

where $X_{CO_2}^a$ and $X_{CO_2}^b$ are the CO₂ equilibrium conversion predicted for the one-step or the two-step process, respectively.

Figure 8 shows CPG as a function of reaction temperature and pressure. The obtained graph can be used as a tool to individuate the optimal operation conditions maximizing the thermodynamic effect in terms of CO₂ conversion. For instance, at reaction pressure of 30 bar, the maximum benefit in terms of X_{CO_2} to carry out the one-step rather than the two-step process can be obtained at ca. 200 °C.

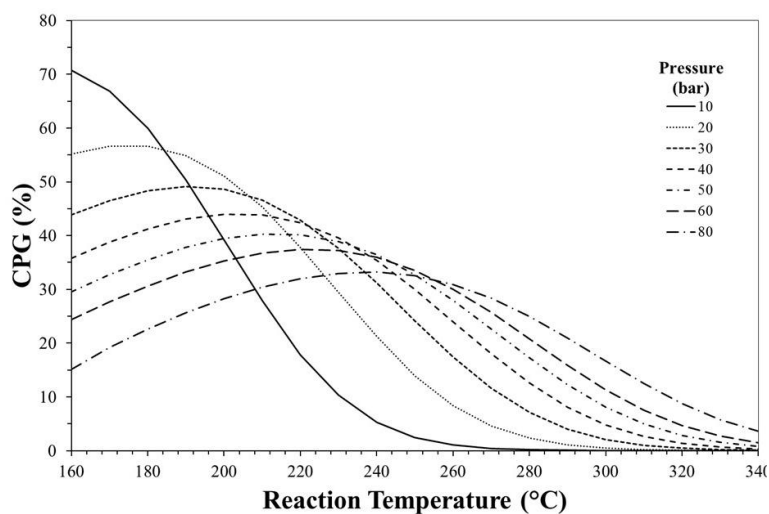


Figure 8. CO₂ conversion percentage gain (CPG) as a function of reaction temperature and pressure.

4. Catalytic Systems for DME Production

As before mentioned, gas phase DME synthesis could be performed in either a two-step process (indirect synthesis) or a single-step process (direct synthesis) [38]. In the conventional indirect synthesis, methanol is first synthesized over a metallic-based catalyst through CO_x hydrogenation [39], then methanol is dehydrated into DME over solid acid catalysts (such as γ -alumina, zeolite, heteropolyacids, ...). On the other hand, in the direct DME synthesis the catalyst functionalities of methanol synthesis and in-situ dehydration are integrated in a bifunctional systems within a single reactor (see Figure 9) and this is an attractive alternative to the two-step process [40–42], also alleviating the thermodynamic constraints of methanol synthesis and leading to higher both CO₂ conversion and DME selectivity [38,39,43]. Moreover, from an industrial point of view, the use of a single reactor should reduce the capital costs for the DME production [44–46].

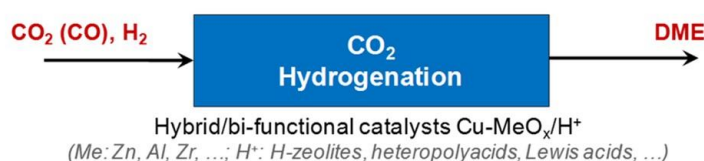


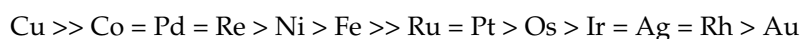
Figure 9. Scheme of the direct synthesis of DME through CO₂ hydrogenation.

It also noteworthy that the real direct DME synthesis product distribution may not correspond to the predicted values by thermodynamics as the product distribution are is also affected by reaction kinetic. Moreover a good understanding of the thermodynamic limitations for direct DME synthesis reaction can be useful for developing new chemical processes and improving the already existing-ones (see Section 3). Anyway, the indirect synthesis is the most diffused process for DME production [47] and also in this case, whatever the process, catalyst properties strongly affect process performances, such as product distribution and deactivation of the catalyst. In this paragraph, the effect of both metal or acid catalyst properties on DME production are discussed, emphasizing on the potential of zeolites as acid catalysts.

4.1. Catalysts for CO₂-to-MeOH Step

In the literature several catalytic systems are claimed as active in the activation of carbon dioxide. Table 3 lists the best performing catalysts, together with the active species used (Cu, Ag, Au, Ni, Pd, Pt), the preparation method and their respective physicochemical and morphological properties [47].

Among these formulations, copper-based catalysts exhibit the best catalytic performance in terms of CO₂ hydrogenation to methanol. In addition, previous studies identified the following order of catalytic activity [48]:



On the whole, this reactivity trend confirms that copper-based systems are the most active ones in the CO₂ activation. In any case, it must be pointed out that catalytic activity strongly depends on metal dispersion, the use of dopants, and the choice of the support. A further key point regarding catalytic hydrogenation from CO₂ rather than syngas is related to the higher oxidation power of CO₂ with respect to CO, thus affecting the active state of the catalyst for methanol synthesis and consequently the methanol formation rate [49]. Therefore, there is a strong influence of the reaction conditions on the overall catalytic behaviour and the need to develop appropriate kinetic models to describe the overall synthesis. This is the basis for a proper modelling of the process and its optimization.

The first commercial catalyst to convert syngas to methanol was produced by BASF (Ludwigshafen, Germany) in 1923 using ZnO-Cr₂O₃ catalyst, active at high temperature (350–400 °C) and pressure (240–350 bar) [44]. However, this catalyst was easily poisoned by impurities of the feed

syngas such as sulfur, chlorine and heavy metals. Imperial Chemical Industry (ICI) introduced a more active and stable Cu/ZnO based catalyst in 1966 [39]. However, although strongly influenced by operating conditions and the preparation methodology, a careful literature data analysis showed that the best systems for the hydrogenation of CO₂ to methanol are Cu/ZrO₂ based [50]. In fact, overcoming the empirical approach, in catalyst design detailed knowledge of the expected catalytic properties is requested, particularly about the control of morphological properties (e.g., total surface area, metal dispersion, crystallinity). This objective can be achieved through a fine design of the catalytic system, adopting a suitable preparation method.

Table 3. Textural and catalytic properties of metal/zirconia catalysts (Reproduced from [47] with permission of The Royal Society of Chemistry, license number: 4254680877107, 23 December 2017). Numbers in the last column refer to references number of reported in Ref. [47].

Catalyst M/ZrO ₂	Prep. ^a	Precursors	BET Surface (m ² ·g ⁻¹)	Metal Surface (m ² ·g ⁻¹)	Product Selectivity ^b			Ref.
					CH ₃ OH	CO	CH ₄	
Cu	impreg.	Copper formate	-	-	-	-	-	11-13
Cu	impreg.	Copper tetrammine	107	1.8	35	65	0	14
Cu	co-prec.	Nitrates	64	-	68	32	0	15,16
Cu	co-prec.	Nitrates	174	7.1	66	34	0	14,17
Cu	co-prec.	Chloride/Sulfate	48.4	-	53	47	0	18
Cu	Ho-prec.	Nitrates	161	3.0	69	31	0	17
Cu	Prec.	Nitrates	86	-	15	57	28	19
Cu	Sol-gel	Acetate	215	-	40	60	0	20
Cu	alloy	Cu ₇₀ Zr ₃₀	47	5.0	64	36	0	21
HT-Cu	Sol-gel, 2	Acetate	128	0.8	100-55			22
HT-Cu	Sol-gel, 1	Acetate	100	-	100-55			22
HT-Cu	Sol-gel, 1	HNO ₃	143	1.3	100-55			22
LT-Cu	Sol-gel, 1	HNO ₃	139	5.0	100-55			22
Cu/CZ1	Sol-gel		253	-	52	47		23
Cu/CZ2	Sol-gel		268	17.8	96	4		23
Cu/CZ3	Sol-gel		241	28.5	97	3		23
Cu/CZ4	Sol-gel		234	31.3	97	3		23
Cu/CZ5	Sol-gel		225	41.2	96	4		23
Cu/ZnO	Sol-gel	Acetates	150	-	64	36	0	20
Cu/Zn 0.1	Ox-co-prec.	Nitrates	39	3.4	36/40			24
Cu/Zn 0.2	Ox-co-prec.	Nitrates	36	14.9	37/46			24
Cu/Zn 0.3	Ox-co-prec.	Nitrates	70	12.6	38/42			24
Cu/Zn 0.4	Ox-co-prec.	Nitrates	45	9.6	37/43			24
Cu/Zn 0.5	Carb-co-prec.				33/38			24
Cu/V	Prec.	Nitrates	185	-	13	67	20	19
Cu/Ag	Co-prec.	Nitrates	281	4.1	81	19	0	25
Ag	Co-prec.	Nitrates	112	-	100	0	0	25
Ag	Impreg.	Nitrates	125	-	70	30	0	26
HT-Ag	Sol-gel, 2	Acetate	99	-	100-55			22
HT-Ag	Sol-gel, 1	Acetate	77	-	100-55			22
HT-Ag	Sol-gel, 1	HNO ₃	125	-	100-55			22
LT-Ag	Sol-gel, 1	HNO ₃	112	-	90-48			22
Au	Co-prec.	HAuCl ₄ /ZrO(NO ₃) ₂	185	-	24	76	0	26,27
Au	alloy	Au ₂₅ Zr ₇₅	47	-	20	74	6	27
Pt	Impreg.	HPtCl ₆ /chloride	-	-	5	2	93	28
Pd	alloy	Pd ₃₃ Zr ₆₇	17	5.6	30	27	43	29
Ni	alloy	Ni ₆₄ Zr ₃₆	8	-	0	0	100	30
Rh	Impreg.	Nitrate/chloride	-	-	5	32	63	31
Rh	Impreg.	Nitrate/chloride	-	-	0	0	100	32,33
Ru	Impreg.	Ru(III)AcAc	-	-	0	0	100	34
Re	Impreg.	-	-	4.1	11	58	29	35
Rh-Mo	Impreg.	Molybdate/chloride	54		0		100	36
Rh-Mo-Li	Impreg.	Molybdate/chloride/nitrate	47		0		100	36
Rh-Mo-K	Impreg.	Molybdate/chloride/nitrate	51		0		100	36
Rh-Mo-Re	Impreg.	Molybdate/chloride/perrhenate	52		0		100	36
Rh-Mo-Co	Impreg.	Molybdate/chloride/nitrate	53		0		100	36
Rh-Mo-Ce	Impreg.	Molybdate/chloride/nitrate	57		0		100	36

^a Alloy: controlled oxidation of amorphous alloys, co-prec.: co-precipitation, impreg.: impregnation, ho-prec.: homogeneous precipitation using urea, sol-gel, 1/2: one/two stage sol-gel methodology, ox-co-prec.: oxalate co-precipitation, carb-co-prec.: carbonate co-precipitation. ^b Note: product selectivities were obtained under different experimental conditions.

Although the Cu-based systems supported on ZnO have been the most studied catalysts for CO₂ hydrogenation, it is clear that the specific activity of copper does not seem apparently influenced by the nature of the carrier oxide. However, previous studies conducted by Chinchén et al. [51] showed that the Zn exerts many functions, giving the best performance among the different tested oxides (Cr₂O₃, SiO₂ and MnO). Zinc oxide acts as a geometrical spacer between Cu nanoparticles and thus plays a pivotal role in maintaining the active Cu metal in optimal dispersion in the Cu/ZnO catalyst, consequently providing a high number of active sites exposed to gaseous reactants [43]. Indeed, beyond to promote the increase of the surface area (especially with alumina), ZnO is enough refractory and it hinders the sintering of copper particles, acting as a dispersing agent of sulphur and chlorides as well, the main poisons for the catalyst. ZnO also plays an important role to maintain an appropriate ratio Cu⁺/Cu⁰, since both states are involved in the synthesis, creating Cu⁺-O-Zn type active sites and thus stabilizing the oxidation state of copper. Behrens et al. [42] have reported that ZnO can promote strong metal-support interaction with Cu species, which induces the formation of “methanol-active copper”. Nakamura et al. [52] found that Zn shows a very good promoting effect in the synthesis of methanol, but not in rWGS reaction. Furthermore, addition of trivalent ions like Al³⁺ into the Cu/ZnO was found to improve stability along with Cu dispersion and metal surface area. Afterwards, a ternary Cu/ZnO/Al₂O₃ (CZA) catalyst started to be used for methanol synthesis operating at moderate pressure ranging from 50 to 100 bar and temperature of ca. 250 °C [37–42].

Although it is unanimously recognized the peculiar functionality both of copper and zinc oxide in the mechanism of CO₂ activation, for a further development of the catalytic system, the need for other metal oxides into the catalyst composition is also required, so to realize multimetallic systems more active than bimetallic catalysts in the formation of MeOH, which will be then dehydrated into DME. Really, many studies have already reported the unique features of various metals added in the catalyst composition as promoters of Cu-Zn based catalysts for the CO₂-to-MeOH hydrogenation reaction, like Al [53–56], Mn [57,58], Cr [59], Au [60], Zr [61–68], Pd [69–71], La [55,72,73], Si [74,75], Ce [55,76], Ga [77,78], V [79], carbon [80–82] or mixtures among them [55,83–86] revealing a superior performance of Zr, Al and Ga in terms of activity, selectivity and stability.

4.2. Catalysts for MeOH-to-DME Step

Dimethyl ether is produced via methanol condensation/dehydration (MeOH-to-DME, MTD):



As discussed above, methanol dehydration is an exothermic reversible reaction that proceeds without mole number variation. For this reason, reaction pressure does not affect conversion equilibrium, while lower reaction temperatures have a thermodynamic benefit toward DME production. Methanol dehydration is an acid-catalyzed reaction and several investigations have been published with the aim to identify an active, selective and stable catalyst at relative low temperature for the above-mentioned thermodynamic advantages. Furthermore, for this technology there are several licensors including Haldor Tospoe, Linde/Lurgi, Toyo Engineering, Uhde, MGC (Mitsubishi Gas Chemical Company, Tokyo, Japan), China Southwestern Research Institute of Chemical Industry and China Energy (Jiutai Group, Shanghai, China).

Depending on catalyst characteristics, methanol dehydration can be carried out in both vapour and liquid phase, with reaction temperature in the range 100–300 °C and pressure up to 20 bar, being γ -Al₂O₃ the most investigated solid acid catalyst, due to its low cost, high surface area, good thermal and mechanical stability. Furthermore, γ -Al₂O₃ shows high selectivity to DME even at high temperature (up to 400 °C) thanks to the presence of weak Lewis acid sites not able to promote side reactions. Unfortunately, these acid characteristics require reaction temperature higher than 250 °C to favour high methanol conversion [85,86], but catalyst activity can be improved by modifying γ -Al₂O₃ surface with silica, aluminium-phosphates, titanium, niobium, boron or others species [87–91].

As demonstrated by several investigations [88,92–95], despite γ -Al₂O₃ offers high selectivity towards DME, it tends to strongly adsorb water produced during the reaction causing deactivation. As above described, an important amount of water is produced especially in the one-pot CO₂-to-DME process. Thus, γ -Al₂O₃, in spite of its several advantages, is not classified as a reliable acid catalyst for DME production by CO₂ hydrogenation.

Heteropolyacids (HPAs) can be also used to catalyze the methanol dehydration step. HPA-type materials can be represented by the formula H_{8-n}[X_n⁺M₁₂O₄₀], where “X” is the central atom (e.g., P⁵⁺, Si⁴⁺, Al³⁺, etc.), “n” is its oxidation state and “M” is the metal ion. Because the high Brønsted acidity displayed from these materials, HPAs offer catalytic performances usually better than other solid catalysts such as zeolites, e.g., ZSM-5, especially at low temperature. Alharbi et al. [96] compared HPAs catalysts with ZSM-5 zeolites with different acidity (Si/Al = 10–120). Results showed that tungsten/phosphorous-containing HPA (HPW) showed a turnover frequency (TOF) of about 53 h⁻¹, while the most active ZSM-5 sample showed a TOF value of about 1 h⁻¹. The authors highlighted that the superior catalytic activity displayed by HPAs can be attributed to a higher acid site strength of these materials. Furthermore, Ladera et al. [97] reported that the accessibility of methanol molecules to proton sites of HPAs can be improved by using TiO₂ as support.

Ion exchange resins (IERS) were also proposed as acid catalysts for methanol dehydration. Divinyl benzene/styrene copolymers are usually used in which sulfonic acid groups are introduced being able to dehydrate methanol to DME. IERS have been considered as attractive catalysts for MTD reaction because the high activity exhibited even at relatively low temperature (<150 °C) [98]. Recent works suggested Nafion resin, Nafion/silica composites or Amberlyst 35/36 as suitable catalysts for the synthesis of DME from methanol [99–101]. On the other hand, the application of ion exchange resins as acid catalysts in the one-pot CO₂-to-DME hydrogenation is hindered by the low thermal stability usually exhibited from these materials under the typical process temperature range (ca. 250 °C) [102].

Methanol Dehydration over Zeolites

Research is now focusing on use of zeolites as catalysts for the methanol dehydration step, especially in view of a potential application as acid catalyst for the one-pot CO₂-to-DME process. Zeolites are applied also in other catalytic processes concerning the reuse of carbon dioxide and production of alternative fuels, such as dry reforming of methane [103–105] and biodiesel production by enzymatic catalysis [106,107].

Zeolites are crystalline aluminosilicates whose catalytic properties are well-known for decades. The ever-growing application of zeolites as catalysts in several industrial processes is mainly due to their unique molecular shape-selectivity resulting from a well-defined regular microporous structure. The possibility of tuning this system of voids (openings and spatial orientation of channels, size and location of cages, etc.) allows to have a catalyst that is able to catalyze the specific reaction pathway. Beside to shape-selectivity, the acid properties of zeolites are of paramount importance in catalysis. Generally, both Brønsted and Lewis type acid sites are simultaneously present in zeolites and their concentration, distribution, strength and location are well known factors affecting the overall activity, product selectivity and deactivation of the catalyst. Such aspects and further insights about the use of zeolites in catalysis are fully reported by Corma [108].

Several investigations [85,109] have been already focused on use of ZSM-5 catalyst for methanol dehydration reaction, exhibiting, unlike γ -Al₂O₃, high resistance toward water adsorption. Furthermore, due to its stronger acid sites (Lewis and/or Brønsted type), ZSM-5 offers high activity in terms of methanol conversion at a relatively low reaction temperature. For instance, Vishwanathan et al. [109] reported a value of methanol conversion of about 80% over H-ZSM-5 at 230 °C, while over γ -Al₂O₃ conversion was just 5%, being necessary to increase the temperature to 320 °C to reach 80%, thus affecting both the process economy and the thermodynamic gain. High activity is also retained because ZSM-5 possesses medium and strong acid sites that allow a fast methanol conversion. Unfortunately, as above mentioned, strong acid sites of zeolites catalyze

also other methanol-involving side reactions, leading to the formation of by-products such as olefins and coke, definitely causing a loss of DME selectivity and deactivation.

The mechanism of DME formation over zeolites by methanol dehydration has been already investigated [110–113], demonstrating that it involves the formation of methoxyl ions by reaction among methanol and the acid sites of the catalyst, followed by combination of another alcohol molecule with methoxy species to form DME (even if the associative mechanism involving two methanol molecules co-adsorbed on the same acid site cannot be excluded). On the contrary, in the temperature range of the direct synthesis of DME (250–280 °C), the strong acid sites of zeolite may convert the methanol into a wide range of hydrocarbons: from olefins (methanol-to-olefins process, MTO) [114,115] to aromatic species that are somehow linked to the olefins production, being involved in the (auto)-catalytic process known as “hydrocarbon pool” mechanism (HCP) [111,115–117]. Under the simultaneous presence of aromatic compounds, acid sites and high temperature, a favourable condition is realized for coke formation, a relevant aspect in MTO. Catalyst structure (channel size and configuration) is the most important factor addressing the pool-molecules formation. At high temperature, characteristic of MTO process, zeolite structures with large cages or 3-D channel system, as SAPO-34, BEA and MFI, promote the formation of aromatic compounds that can be entrapped in the structure or diffuse out. The most common aromatic species are in the class of poly-methylbenzenes, depending on the catalyst channel size: tri-methylbenzene is the most active species on MFI, while hexa-methylbenzene is the most active for olefins formation in the large cages of SAPO-34 and BEA [118]. These molecules are also considered as coke precursors and it is important to notice that they can be produced also in the lowest temperature range of MeOH-to-DME reaction. Under such conditions these poly-methylbenzenes do not act as co-catalysts in HCP (because of the low temperature), accumulating in the structure as carbon deposits. Furthermore, in the case of either DME or olefins synthesis, it is well known that zeolite deactivation mainly comes from the coke deposition inducing pore blocking. In addition, it has been demonstrated that both catalyst structure and acidity strongly affect the mechanism of coke formation, in terms of composition, quantity and location. Campelo et al. [119] reported a comparison between several silico-aluminophosphates with different channel configuration (1-, 2- and 3-dimension), showing that on a 3-dimensional structure (as SAPO-34), the oligomers formed in the channels can migrate to the big cages of this structure, where react over strong acid sites so leading to the formation of heavier oligomers and aromatics that cannot back to the channels, causing a rapid catalyst deactivation for pore blocking. On the other hand, deactivation of 1-dimensional large channels (as SAPO-5) is due to the adsorption of multi-branched chains on the strong acid sites, also causing blocking of the pore system. Structures with both small/medium channels and cages, as MFI type, do not permit trapping of heavy compounds inside the crystal and coke is preferably formed on the external surface of crystals, so that catalyst deactivation occurs by coke deposition on the mouth of the channels [120,121]. Catalyst deactivation rate is also affected by crystal morphology: small or hierarchical crystals exhibit higher resistance to deactivation by coke deposition than large crystals with microporous texture [122,123]. On small 1-D structures, as MTF, no hydrocarbon pool mechanism is observed even at high temperature (400 °C) and DME is the only product detected in reactor out-stream; nevertheless this structure exhibits fast deactivation over time [124] as consequence of carbon deposition. Therefore, catalyst structure may play a key role on product selectivity, inhibiting either the hydrocarbon pool mechanism or the formation of coke precursors with the aim to increase the catalyst stability overtime.

Recently, several studies were dedicated to study the effect of zeolites structure on catalytic performances during methanol-to-DME reaction step at reaction temperature of direct synthesis (<280 °C).

On 2017, Catizzone et al. [125] studied methanol dehydration reaction on several zeolites (or molecular sieves) having different channel orientation (1-, 2- and 3-dimensional channel orientation) and channel openings (from 8- to 12-membered rings). Results clearly showed how the voids system of zeolites is of paramount importance for this reaction. 1-dimensional zeolites with large pore openings

(e.g., MTW or MOR) showed high selectivity towards DME (at 240 °C), but a fast deactivation rate was observed, attributable to pore blocking by coke deposition. On the contrary, by using 1-dimensional zeolite with medium-pore openings (such as TON), both a higher stability towards deactivation and lower coke deposition was observed. Zeolites with 3-dimensional channel orientation (i.e., MFI, BEA or SAPO-34) were also investigated by the authors [125,126]. Despite the small channel openings of SAPO-34 (about 3.8 Å) conferring high selectivity towards DME, this catalyst was rapidly deactivated by coke formed and deposited into the large 3-dimensional channel intersections (about 7.4 Å large), so preventing reactant diffusion inside the crystal. On the contrary, when channel openings and intersections have similar size (e.g., in the case of BEA or MFI structure) a higher stability was observed, even if by-products (e.g., C₂=-C₆=) were detected in the reaction out-stream and a high coke deposition rate was observed [127].

Coke deposited during methanol dehydration to DME over zeolites mainly consists of polymethylbenzenes (PMB, ranging from xylenes to hexamethylbenzene) with a grade of substitution that is a function of the channel system. For instance, the 1-D medium pore channel system of TON inhibits the formation of PMB heavier than tri-methyl benzene; on the contrary, despite the similar channel openings of TON, EUO-type structure accommodates also hexa-methyl benzene due to the presence of side-pockets large enough to permit the formation of this molecule. Zeolites with large pore system, such as beta, also allows deposition of polycyclic species, while carbon phase deposited on FER-type crystals selectively consists of tetramethylbenzene compound probably located in ferrierite cages [125].

Coke formation can be reduced by post-synthesis treatment or by a careful tailoring of the textural properties. A dual pore size distribution (e.g., micro- and mesopores) is a reliable configuration to reduce coke formation and postpone catalyst deactivation during methanol dehydration. Tang et al. [128] reported that a ZSM-5/MCM-41 composite material with both microporous and mesoporous allows to obtain higher activity and higher stability than ZSM-5 with only microporous structure. Similar results were obtained by Rutkowska et al. [129] which showed that hierarchical ZSM-5 material (interconnected micro-/mesopores) exhibits a lower coke formation rate than microporous ZSM-5.

On the whole, several results suggest FER zeolite as a reliable catalyst to selectively transform methanol to DME [125,130,131]. Thanks to its 8-/10-membered ring 2-dimensional channel system, FER structure shows a high DME selectivity, a slow coke deposition and a high resistance to deactivate.

Beside the structure, the acidity properties of zeolites also strongly affect the catalytic behaviour of these materials. High catalytic performances, in terms of DME selectivity, were obtained by decreasing the acid site strength, upon modification of the zeolite surface [132,133], or by decreasing total acidity [109,134,135].

Kim et al. [132] studied methanol dehydration reactions over ZSM-5 zeolites impregnated with different γ -Al₂O₃ loading and compared the catalysts in terms of operative temperature range (OTR), defined as the temperature range giving methanol conversion higher than 50% and DME selectivity higher than 99%. The authors found that OTR of 210–310 °C and 320–370 °C were evaluated for bare ZSM-5 and γ -Al₂O₃ confirming that the zeolite is more active but less selective than γ -Al₂O₃. On the contrary, a hybrid catalyst γ -Al₂O₃/ZSM-5, containing 70% γ -Al₂O₃, exhibited an OTR of 230–380 °C showing, therefore, higher activity than γ -Al₂O₃, but also higher selectivity than both γ -Al₂O₃ and bare ZSM-5 thanks to the suitable dilution of strong acid sites of zeolite after impregnation.

Similar results were obtained by other authors by impregnation of ZSM-5 catalyst with sodium, magnesium, zinc or zirconium [133,134]. The authors showed that metal loading decreases strong acidity and increases weak acidity, forming a catalyst less active towards hydrocarbon formation. For instance, Khandan et al. [134] reported that DME yield increased from 53% to 93% after impregnation of ZSM-5 with zirconium; moreover, stability tests showed that resistance towards deactivation was also improved.

Acidity in zeolites can be also decreased by reducing the aluminium content or increasing the Si/Al ratio [135,136]. In this concern, Hassanpour et al. [135] prepared ZSM-5 catalysts in a wide range

of Si/Al ratio (Si/Al = 25–250) and tested them in methanol conversion at 300 °C. The authors found that by-products formation (e.g., ethylene, propylene) decreases as the Si/Al increases, obtaining higher DME selectivity for catalysts with lower total acidity.

Catizzone et al. [131] have recently reported some aspects concerning the role of acid sites of FER-type zeolites by preparing catalysts with different Si/Al ratio. The authors reported that higher methanol conversion levels can be achieved over FER zeolites with higher aluminum content, but experimental evidences also demonstrated that lattice Lewis acid sites are more active than Brønsted sites even if a reaction temperature lower than 260–280 °C should be adopted in order to prevent by-products formation (especially methane). As previously discussed about thermodynamic aspects, a good catalyst for methanol dehydration step should promote high methanol conversion at temperature lower than 240–260 °C. The superiority of FER zeolite over γ -Al₂O₃ and several other zeolites at temperature lower than 240 °C was demonstrated recently [125]. In this paper, the authors showed that, at only 200 °C, methanol conversion was about 82% over FER with a 100% of DME selectivity, while a methanol conversion level of 25% only was observed for commercial γ -Al₂O₃. As discussed below, recent studies consider FER-type zeolite as a very promising acid functionality for preparing an attractive hybrid catalyst for CO₂ hydrogenation to DME.

4.3. Catalysts for One-Pot CO₂ Hydrogenation to DME

The catalyst for the direct CO₂-to-DME conversion should be able to efficiently catalyze both methanol synthesis and its dehydration, minimizing the yield of CO formed by the Reverse Water Gas Shift (rWGS) side reaction and possible hydrocarbons from methanol conversion. A huge amount of water formed during CO₂ hydrogenation to DME thermodynamically limits both formation and dehydration of methanol, causing a DME yield lower than that obtained via CO hydrogenation [85].

In this concern, the acid catalyst must be stable in presence of water and the acid sites must be well distributed and not too strong in order to inhibit hydrocarbons formation [85,89,137–144]. In this sense, as above described, zeolites seem to offer the highest versatility in terms of higher number of acid sites, water resistance and shape-selectivity towards the desired compound. A list of some results [77,145–157] concerning the one-pot CO₂ hydrogenation to DME is reported in Table 4.

The first studies on hybrid/bifunctional catalytic systems active in the direct hydrogenation reaction of CO₂ dealt with the use of physical mixtures between a methanol synthesis catalyst (MSC) and an acid system, typically a Cu-ZnO-Al₂O₃ system for the synthesis of MeOH and γ -Al₂O₃ or zeolites as acid solids for the dehydration of MeOH (see Section 4.2).

Zeolites, in particular, have shown greater efficiency than γ -Al₂O₃ as acid components of the bifunctional catalyst, considering that the possibility of modulating acidity (in terms of number, type and strength of acid sites) enables direct synthesis of DME at low temperatures, where the formation of methanol is thermodynamically favored. For instance, Naik et al. [145] compared the catalytic activity of hybrid catalysts prepared by mechanical mixing of MSC and γ -Al₂O₃ or ZSM-5 (Si/Al = 60). Catalytic tests carried out in a fixed-bed reactor at 260 °C and 5 MPa revealed that MSC/ZSM-5 exhibits a superior catalytic behaviour than MSC/ γ -Al₂O₃ in terms of CO₂ conversion (ca. 30% vs. ca. 20%), DME selectivity (ca. 75% vs. ca. 5%) and stability. As a conclusion, DME yield was about 20% over MSC/ZSM-5 and lower than 1% over MSC/ γ -Al₂O₃ suggesting that γ -Al₂O₃ cannot be considered as a valuable acid catalyst for the one-pot CO₂-to-DME process.

Table 4. Recent investigated catalysts for one-pot CO₂-to-DME process. PM: physical mixing; WM: wet mixing; CP: co-precipitation; IM: impregnation; GHSV: Gas Hourly Space Velocity; P: reaction pressure; T: reaction temperature; X_{CO₂}: conversion of CO₂; Y_i: carbon-basis yield of *i*-product.

Catalyst	Preparation Method	H ₂ /CO ₂	GHSV (NmL·g ⁻¹ ·h ⁻¹)	P;T (MPa; °C)	X _{CO₂} (%)	Y _{CO} (%)	Y _{MeOH} (%)	Y _{DME} (%)	Ref.
Cu/Zn/Al HZSM5	PM	3	3000	5;260	31	2	9.3	19	[145]
Cu/Zn/Al γ-Al ₂ O ₃					20	11.6	8	0.4	
Cu/Zn/Al/Zr ZSM5	WM	3	3100	3;260	24.1	7	10.6	6.4	[146]
Cu/Zn/Zr Ga-Sil1	CP	3	1200	3;250	19.0	6.4	4	8.6	[147]
Cu/Ti/Zr ZSM5	WM	3	1500	3;250	15.6	6.1	2.0	7.4	[148]
Cu/Zn/Zr/V ZSM5	CP	3	1500	3;270	32.5	9.1	4.3	19.1	[77]
Cu/Zn/Al/Zr ZSM5	PM	3	6000	5;270	27.5	-	5.0	16	[149]
Cu/Zn/Al/La ZSM5	PM	3	3000	3;250	43.8	0.11	1.9	31.2	[150]
Cu/Mo ZSM5	IM	2	1500	3;240	12.4	2	0.7	9.5	[151]
Cu/Zn/Zr/Pd ZSM5	CP	3	1800	3;200	18.7	2.4	2.5	13.8	[152]
Cu/Zn/Al ZSM5+CNTs	PM	3	1800	3;260	46.2	8.9	16.4	21	[153]
Cu/Zn/Zr FER	CP	3	8800	5;260	23.6	9.2	3.5	10.6	[154]
Cu/Zn/Al ZSM5	CP	3	750	4;275	35			23	[155]
Cu/Zn/Al γ-Al ₂ O ₃					40	-	-	10	
Cu/Zn/Al Amorphous silica-alumina	CP	3	1800	3;270	47.1	12.3	14.7	20.1	[156]
Cu/Fe/Zr ZSM5	PM	5	1500	3;260	28.4	2.2	4.2	18.3	[157]

Compared to the conventional mechanical mixing between a methanol synthesis catalyst and a zeolite, the generation of metal oxide and acid sites in a single system is capable of improving the conversion of CO₂, enabling even higher rates of formation/dehydration of methanol on the neighbouring surface sites. Different strategies have been applied to prepare the bifunctional catalysts for the direct DME synthesis. For instance, methods including impregnation, co-precipitation [158–162] or sol-gel steps (or their combinations) [44,163] and even more sophisticated approaches leading to core-shell catalyst structures [164–166] have been reported. Nevertheless, there are different opinions on the efficiency of bifunctional catalysts in comparison to admixed systems. Sun et al. prepared bifunctional catalysts by coprecipitation-sedimentation of a ZrO₂-doped CZA-component on an H-ZSM5 zeolite [152,167]. According to that, bifunctional catalysts lead to high CO-conversions because the two types of active sites are in close contact with each other. This enables the generation of DME directly from an adsorbed methoxy-species without the intermediary synthesis of methanol.

Ge et al. also concluded that both active sites need to be in close contact so that a synergistic effect can be achieved, which leads to higher catalytic activity [44]. However, Ge et al. stressed that coverage of both active sites during catalyst synthesis needs to be avoided.

A coverage of the active sites leads to a drop of activity due to the synthesis of inactive species and due to a decrease in active surface area. García-Trenco et al. stated that admixed catalyst systems are superior to bifunctional systems [168]. Therefore, the preparation procedure of bifunctional catalysts can lead to a decrease of surface area due to a pores blockage. However, it is also stated that further interactions between the two active components, which have not been elucidated yet, might influence catalyst activity as well.

Although the design of the catalytic system ideal for the hydrogenation of CO₂ does not require properties such as selectivity of shape and/or size, due to the small size of the molecules involved, the zeolites still have a high potential expressed through multiple properties, such as tunable acidity, high surface area, microporosity or supporting properties, which represent the fundamental reasons featuring these unique structures as metal and/or metal-oxide carriers in most of current catalytic systems.

Frusteri et al. [161] have recently investigated the role of acid sites of hybrid catalysts prepared via gel-oxalate precipitation of CuZnZr precursors of ZSM-5 crystals with a Si/Al ratio in the range 27–127. Results displayed that acidity of zeolite must be carefully tuned aiming at achieving a compromise between catalytic activity and resistance to deactivation by water. In particular, ZSM-5 with high Si/Al ratio (e.g., 127) showed high resistance in presence of water but low capacity to dehydrate methanol, while more acidic samples (e.g., ZSM-5 with Si/Al ratio of 27) offers high methanol conversion but poor water resistance and low DME selectivity. The authors found that, for the ZSM-5 zeolite, a Si/Al ratio of 38 showed the best performance in terms of CO₂ conversion, DME yield and water resistance.

Beside acidity, the textural properties of zeolite crystals also strongly affect the catalytic behaviour of hybrid catalysts. In this regard, the one-pot CO₂-to-DME reaction in the presence of hybrid grains prepared via co-precipitation of CuZnZr precursors over zeolite crystals with different channel systems (i.e., MOR, FER and MFI) was recently investigated [158]. The microscopy analysis of hybrid grains revealed that zeolite crystal features strongly affect the metal-oxide(s) distribution, producing a very homogenous distribution over lamellar FER-type crystals and a formation of metal clusters on the other zeolite crystals. Catalytic results revealed that DME productivity followed the trend: CuZnZr/FER > CuZnZr/MOR > CuZnZr/MFI, and the authors related the superior catalytic activity of FER-based catalyst to lower mass transfer limitations offered by anchorage of metal-oxide clusters on the lamellar crystals typical of FER zeolite as well as to a larger population of Lewis basic sites generated on FER surface able to activate carbon dioxide and promoting its conversion. Nevertheless, an important deactivation of the catalyst was observed during time-on-stream tests.

The hybrid catalysts developed so far generally tend to suffer deactivation by either coke deposition or metal sintering or poisoning from contaminants present in the reaction stream leading to the blockage of active sites [169,170]. As before mentioned, for hydrocarbon reactions over zeolites,

deactivation is mainly attributed to two main mechanisms: (1) acid site coverage which deactivates the catalyst by coke adsorption; (2) pore blockage due to deposition of carbonaceous compounds in cavities or channel intersections that makes pores inaccessible [171]. In addition, it is well known that coke formation on zeolites is a shape-selective process. Under comparable conditions, large-pore zeolites are more susceptible to deactivation by coke deposition than medium-pore zeolites [172]. Although H-ZSM-5 is not sensitive to water [173,174], it shows high activity for the transformation of DME into hydrocarbon byproducts. These hydrocarbons can further evolve into heavy structures (coke) and consequently can block the zeolite pores and cause its deactivation, as previously discussed. However, this deactivation is slow due to the high partial pressure of hydrogen that attenuates the mechanism of coke formation [148]. This phenomenon can be controlled by employing a suitable concentration of Na in the zeolite in order to moderate the number of Brønsted sites and to reduce the acid strength of the H-ZSM-5 zeolite [170]. The addition of Silicalite-1 shell to the ZSM-5 zeolite is also considered as an efficient method for improving the resistance to the carbon formation [174]. As a rule, the reactor configuration strongly affects catalyst deactivation: considering that the reactors mostly used in the production of DME are slurry or fixed bed reactors, the bifunctional catalysts were seen to deactivate more quickly in slurry rather than in fixed-bed reactors [175].

These examples show that a deeper understanding of the underlying mechanisms and interactions among the active components both in admixed and in bifunctional catalysts is necessary. Furthermore, the influence of the catalyst composition as well as the main features controlling catalytic activity and stability should be studied in more detail, so that a comparison of the catalyst performance independent of the adopted preparation method will be possible.

5. Conclusions and Perspectives on the Catalyst Development

Zeolites are unique materials with huge catalytic potential in several industrial processes, recently generating great research interest as dehydration components in the synthesis of DME, starting not only from methanol, but even from CO₂-rich streams recycled for hydrogenation. From the analysis of the thermodynamic equilibriums involved in the hydrogenation of CO₂, it has been demonstrated that the production of DME is favoured at high pressure and low temperature for achieving both high conversion and DME yield. During CO₂-to-DME hydrogenation reaction ($P \geq 30$ bar; $T \leq 260$ °C) the use of zeolites does not imply to simply exploit their typical shape/size selectivity, but other important features are involved, such as tunable solid acidity, high surface area, microporosity or loading property, representing the fundamental reasons why these unique structures are utilized as carriers of metals and/or metal-oxides.

Generally, a mechanical mixture of mixed oxides (containing Cu as active species for the synthesis of methanol) and a zeolite, typically ZSM-5, have been mainly proposed as an effective catalytic system. However, recent papers have claimed alternative zeolite structures as more suitable for the process, evidencing how the zeolite topology significantly affects the physicochemical properties of the catalysts as well as their catalytic performance. In particular, some fundamental aspects have been indicated as crucial for high process productivity: (i) the zeolite must be stable in presence of water; (ii) the formation of olefins should be inhibited; (iii) the acid sites must be well distributed and of suitable strength. Moreover, the performance of multi-site systems for the direct conversion of CO₂ into DME has been also proved, so demonstrating the possibility to integrate the two methanol-synthesis and methanol-dehydration functionalities at level of single grain during preparation. Apart from the need of optimal experimental parameters, the crucial issue for preparing a high-active hybrid catalyst is optimizing the formulation and interaction of the different metallic, oxide(s) and acidic components, so to realize a punctual mix of surface sites necessary for the primary formation of methanol, followed by its dehydration to DME on the acid sites of the zeolite. Overall, in the perspective to develop an active and stable multi-site catalyst for DME production via CO₂ hydrogenation, the concurrence of textural, structural and surface factors must be adequately balanced.

Acknowledgments: Part of this work was realized within the bilateral agreement of Scientific and Technological Cooperation CNR-MTA/HAS (Hungarian Academy of Sciences).

Author Contributions: E.C. wrote the paragraphs 1, 2 and 3, performed thermodynamics calculations and revised the manuscript; G.B. and M.M. conceived the structure of the review, wrote abstract and paragraphs 4 and 5 and revised the manuscript; F.F. and G.G. revised the manuscript and were managers of the research project.

Conflicts of Interest: The authors declare no conflict of interest.

References

1. Zhou, P.; Wang, M. Carbon dioxide emissions allocation: A review. *Ecol. Econ* **2016**, *125*, 47–59. [[CrossRef](#)]
2. De Conik, H.; Benson, S.M. Carbon dioxide capture and storage: Issues and prospects. *Annu. Rev. Environ. Resour.* **2014**, *39*, 243–270. [[CrossRef](#)]
3. Chianese, D.S.; Rotz, C.A.; Richard, T.L. Simulation of carbon dioxide emission from dairy farms to assess greenhouse gas reduction strategies. *Trans. ASABE* **2009**, *52*, 1301–1312. [[CrossRef](#)]
4. Tseng, S.-C.; Hung, S.-W. A strategic decision-making model considering the social costs of carbon dioxide emissions for sustainable supply chain management. *J. Environ. Manag.* **2014**, *133*, 315–322. [[CrossRef](#)] [[PubMed](#)]
5. Olah, G.A. Beyond oil and gas: The methanol economy. *Angew. Chem. Int. Ed.* **2005**, *44*, 2636–2639. [[CrossRef](#)] [[PubMed](#)]
6. Arcoumanis, C.; Bae, C.; Crookes, R.; Kinoshita, E. The potential of di-methyl ether (DME) as an alternative fuel for compression-ignition engines: A review. *Fuel* **2008**, *87*, 1014–1030. [[CrossRef](#)]
7. Ogawa, T.; Inoue, N.; Shikada, T.; Ohno, Y. Direct dimethyl ether synthesis. *J. Nat. Gas Chem.* **2003**, *12*, 219–227.
8. Cheng, C.; Zhang, H.; Ying, W.; Fang, D. Intrinsic kinetics of one-step dimethyl ether synthesis from hydrogen-rich synthesis gas over bi-functional catalyst. *Korean J. Chem. Eng.* **2011**, *28*, 1511–1517. [[CrossRef](#)]
9. Trippe, F.; Frohling, M.; Schultmann, F.; Stahl, R.; Henrich, E.; Dalai, A. Comprehensive techno-economic assessment of dimethyl ether (DME) synthesis and Fischer–Tropsch synthesis as alternative process steps within biomass-to-liquid production. *Fuel Process. Technol.* **2013**, *106*, 577–586. [[CrossRef](#)]
10. Basu, A.; Fleisch, T.H.; McCarthy, C.I.; Udovich, C.A. Process and Fuel for Spark Ignition Engines. U.S. Patent 5,632,786, 27 May 1997.
11. Centi, G.; Quadrelli, E.A.; Perathoner, S. Catalysis for CO₂ conversion: A key technology for rapid introduction of renewable energy in the value chain of chemical industries. *Energy Environ. Sci.* **2013**, *6*, 1711–1731. [[CrossRef](#)]
12. Tamagnini, P.; Axelsson, R.; Lindberg, P.; Oxelfelt, F.; Wunschiers, R.; Lindblad, P. Renewable hydrogen production. *Microbiol. Mol. Biol. Rev.* **2006**, *66*, 1–20. [[CrossRef](#)]
13. Chaubey, R.; Sahu, S.; James, O.O.; Maity, S. A review on development of industrial processes and emerging techniques for production of hydrogen from renewable and sustainable sources. *Renew. Sustain. Energy Rev.* **2013**, *23*, 443–462. [[CrossRef](#)]
14. Parthasarathy, P.; Narayanan, K.S. Hydrogen production from steam gasification of biomass: Influence of process parameters on hydrogen yield—A review. *Renew. Energy* **2014**, *66*, 570–579. [[CrossRef](#)]
15. Kalinci, Y.; Hepbasli, A.; Dincer, I. Biomass-based hydrogen production: A review and analysis. *Int. J. Hydrog. Energy* **2009**, *34*, 8799–8817. [[CrossRef](#)]
16. Ni, M.; Leung, M.K.H.; Leung, D.Y.C.; Sumathy, K. A review and recent developments in photocatalytic water-splitting using TiO₂ for hydrogen production. *Renew. Sustain. Energy Rev.* **2007**, *11*, 401–425. [[CrossRef](#)]
17. Ismail, A.A.; Bahnemann, D.W. Photochemical splitting of water for hydrogen production by photocatalysis: A review. *Sol. Energy Mater. Sol. Cells* **2014**, *128*, 85–101. [[CrossRef](#)]
18. Álvarez, A.; Bansode, A.; Urakawa, A.; Bavykina, A.V.; Wezendonk, T.A.; Makkee, M.; Gascon, J.; Kapteijn, F. Challenges in the Greener Production of Formates/Formic Acid, Methanol, and DME by Heterogeneously Catalyzed CO₂ Hydrogenation Processes. *Chem. Rev.* **2017**, *117*, 9804–9838. [[CrossRef](#)] [[PubMed](#)]
19. Semelsberger, T.A.; Borup, R.L.; Greene, H.L. Dimethyl ether (DME) as an alternative fuel. *J. Power Sources* **2006**, *156*, 497–511. [[CrossRef](#)]
20. Park, S.H.; Lee, C.S. Combustion performance and emission reduction characteristics of automotive DME engine system. *Prog. Energy Combust. Sci.* **2013**, *39*, 147–168. [[CrossRef](#)]

21. Sidhu, S.; Graham, J.; Striebich, R. Semi-volatile and particulate emissions from the combustion of alternative diesel fuels. *Chemosphere* **2001**, *42*, 681–690. [[CrossRef](#)]
22. Kim, M.Y.; Yoon, S.H.; Ryu, B.W.; Lee, C.S. Combustion and emission characteristics of DME as an alternative fuel for compression ignition engines with a high pressure injection system. *Fuel* **2008**, *87*, 2779–2786. [[CrossRef](#)]
23. Egnell, R. *Comparison of Heat Release and NO_x Formation in a DI Diesel Engine Running on DME and Diesel Fuel*; SAE Technical Paper 2001-01-0651; SAE 2001 World Congress: Detroit, MI, USA, 2001. [[CrossRef](#)]
24. Teng, H.; McCandless, J.C.; Schneyer, J.B. *Thermochemical Characteristics of Dimethyl Ether—An Alternative Fuel for Compression-Ignition Engines*; SAE Technical Paper 2001-01-0154; SAE 2001 World Congress: Detroit, MI, USA, 2001. [[CrossRef](#)]
25. Fleisch, T.H.; Basu, A.; Gradassi, M.J.; Massin, J.G. Dimethyl ether: A fuel for the 21st century. *Stud. Surf. Sci. Catal.* **1997**, *107*, 117–125. [[CrossRef](#)]
26. Gupta, K.K.; Rehman, A.; Sarviya, R.M. Bio-fuels for the gas turbine: A review. *Renew. Sustain. Energy Rev.* **2010**, *14*, 2946–2955. [[CrossRef](#)]
27. Lee, M.C.; Seo, S.B.; Chung, J.H.; Joo, Y.J.; Ahn, D.H. Combustion performance test of a new fuel DME to adapt to a gas turbine for power generation. *Fuel* **2008**, *87*, 2162–2167. [[CrossRef](#)]
28. Lee, M.C.; Seo, S.B.; Chung, J.H.; Joo, Y.J.; Ahn, D.H. Industrial gas turbine combustion performance test of DME to use as an alternative fuel for power generation. *Fuel* **2009**, *88*, 657–662. [[CrossRef](#)]
29. Lee, M.C.; Yoon, Y. Development of a gas turbine fuel nozzle for DME and a design method thereof. *Fuel* **2012**, *102*, 823–830. [[CrossRef](#)]
30. Haryanto, A.; Fernando, S.; Murali, N.; Adhikari, S. Current status of hydrogen production techniques by steam reforming of ethanol: A review. *Energy Fuels* **2005**, *19*, 2098–2106. [[CrossRef](#)]
31. Ghenciu, A.F. Review of fuel processing catalysts for hydrogen production in PEM fuel cell systems. *Curr. Opin. Solid State Mater. Sci.* **2002**, *6*, 389–399. [[CrossRef](#)]
32. Palo, D.R.; Dagle, R.A.; Holladay, J.D. Methanol steam reforming for hydrogen production. *Chem. Rev.* **2007**, *107*, 3992–4021. [[CrossRef](#)] [[PubMed](#)]
33. Takeishi, K.; Suzuki, H. Steam reforming of dimethyl ether. *Appl. Catal. A* **2004**, *260*, 111–117. [[CrossRef](#)]
34. Vicente, J.; Gayubo, A.G.; Ereña, J.; Aguayo, A.T.; Olazar, M.; Bilbao, J. Improving the DME steam reforming catalyst by alkaline treatment of the HZSM-5 zeolite. *Appl. Catal. B* **2013**, *130–131*, 73–83. [[CrossRef](#)]
35. Gazsi, A.; Ugrai, I.; Solymosy, F. Production of hydrogen from dimethyl ether on supported Au catalysts. *Appl. Catal. A* **2011**, *391*, 360–366. [[CrossRef](#)]
36. Semelsberger, T.A.; Ott, K.C.; Borup, R.L.; Greene, H.L. Generating hydrogen-rich fuel-cell feeds from dimethyl ether (DME) using physical mixtures of a commercial Cu/Zn/Al₂O₃ catalyst and several solid-acid catalysts. *Appl. Catal. B* **2006**, *65*, 291–300. [[CrossRef](#)]
37. Jeong, J.W.; Ahn, C.-I.; Lee, D.H.; Um, S.H.; Bae, J.W. Effects of Cu–ZnO Content on Reaction Rate for Direct Synthesis of DME from Syngas with Bifunctional Cu–ZnO/γ-Al₂O₃ Catalyst. *Catal. Lett.* **2013**, *143*, 666–672. [[CrossRef](#)]
38. Asthana, S.; Samanta, C.; Bhaumik, A.; Banerjee, B.; Voolapalli, R.K.; Saha, B. Direct synthesis of dimethyl ether from syngas over Cu-based catalysts: Enhanced selectivity in the presence of MgO. *J. Catal.* **2016**, *334*, 89–101. [[CrossRef](#)]
39. Wender, I. Reactions of synthesis gas. *Fuel Process. Technol.* **1996**, *48*, 189–297. [[CrossRef](#)]
40. Huang, M.H.; Lee, H.M.; Liang, K.C.; Tzeng, C.C.; Chen, W.H. An experimental study on single-step dimethyl ether (DME) synthesis from hydrogen and carbon monoxide under various catalysts. *Int. J. Hydrog. Energy* **2015**, *40*, 13583–13593. [[CrossRef](#)]
41. Sousa-Aguiar, E.F.; Appel, L.G.; Mota, C. Natural gas chemical transformations: The path to refining in the future. *Catal. Today* **2005**, *101*, 3–7. [[CrossRef](#)]
42. Bae, J.W.; Potdar, H.S.; Kang, S.-H.; Jun, K.-W. Coproduction of methanol and dimethyl ether from biomass-derived syngas on a Cu–ZnO–Al₂O₃/γ-Al₂O₃ hybrid catalyst. *Energy Fuels* **2008**, *22*, 223–230. [[CrossRef](#)]
43. Aguayo, A.T.; Ereña, J.; Mier, D.; Arandes, J.M.; Olazar, M.; Bilbao, J. Kinetic Modeling of Dimethyl Ether Synthesis in a Single Step on a CuO–ZnO–Al₂O₃/γ-Al₂O₃ Catalyst. *Ind. Eng. Chem. Res.* **2007**, *46*, 5522–5530. [[CrossRef](#)]

44. Ge, Q.; Huang, Y.; Qiu, F.; Li, S. Bifunctional catalysts for conversion of synthesis gas to dimethyl ether. *Appl. Catal. A* **1998**, *167*, 23–30. [[CrossRef](#)]
45. Wang, Z.; Wang, J.; Diao, J.; Jin, Y. The synergy effect of process coupling for dimethyl ether synthesis in slurry reactors. *Chem. Eng. Technol.* **2001**, *24*, 507–511. [[CrossRef](#)]
46. Fleisch, T.H.; Basu, A.; Sills, R.A. Introduction and advancement of a new clean global fuel: The status of DME developments in China and beyond. *J. Nat. Gas Sci. Eng.* **2012**, *9*, 94–107. [[CrossRef](#)]
47. Wambach, J.; Baiker, A.; Wokaum, A. CO₂ hydrogenation over metal/zirconia catalysts. *Phys. Chem. Chem. Phys.* **1999**, *1*, 5071–5080. [[CrossRef](#)]
48. Sugawa, S.; Sayama, K.; Arakawa, H. Methanol synthesis from CO₂ and H₂ over silver catalyst. *Energy Convers. Manag.* **1995**, *36*, 665–668. [[CrossRef](#)]
49. Centi, G.; Perathoner, S. Advances in Catalysts and Processes for Methanol Synthesis from CO₂. In *CO₂: A Valuable Source of Carbon*; Springer: London, UK, 2013; pp. 147–169.
50. Koppel, R.A.; Stocker, C.; Baiker, A. Copper-and silver-zirconia aerogels: Preparation, structural properties and catalytic behavior in methanol synthesis from carbon dioxide. *J. Catal.* **1998**, *179*, 515–527. [[CrossRef](#)]
51. Chinchin, G.C.; Mansfield, K.; Spencer, M.S. The methanol synthesis-how does it work. *Chemtech* **1990**, *11*, 692–699.
52. Nakamura, J.; Nakamura, I.; Uchijima, T.; Kanai, Y.; Watanabe, T. Methanol synthesis over a Zn-deposited copper model catalyst. *Catal. Lett.* **1995**, *31*, 325–331. [[CrossRef](#)]
53. Wang, X.; Zhang, H.; Li, W. In situ IR studies on the mechanism of methanol synthesis from CO/H₂ and CO₂/H₂ over Cu-ZnO-Al₂O₃ catalyst. *Korean J. Chem. Eng.* **2010**, *27*, 1093–1098. [[CrossRef](#)]
54. Samei, E.; Taghizadeh, M.; Bahmani, M. Enhancement of stability and activity of Cu/ZnO/Al₂O₃ catalysts by colloidal silica and metal oxides additives for methanol synthesis from a CO₂-rich feed. *Fuel Process. Technol.* **2012**, *96*, 128–133. [[CrossRef](#)]
55. Gao, P.; Li, F.; Zhao, N.; Xiao, F.; Wei, W.; Zhong, L.; Sun, Y. Influence of modifier (Mn, La, Ce, Zr and Y) on the performance of Cu/Zn/Al catalysts via hydrotalcite-like precursors for CO₂ hydrogenation to methanol. *Appl. Catal. A* **2013**, *468*, 442–452. [[CrossRef](#)]
56. Słoczyński, J.; Grabowski, R.; Kozłowska, A.; Olszewski, P.; Lachowska, M.; Skrzypek, J.; Stoch, J. Effect of Mg and Mn oxide additions on structural and adsorptive properties of Cu/ZnO/ZrO₂ catalysts for the methanol synthesis from CO₂. *Appl. Catal. A* **2003**, *249*, 129–138. [[CrossRef](#)]
57. Fujiwara, M.; Ando, H.; Tanaka, M.; Souma, Y. Hydrogenation of carbon dioxide over Cu-Zn-Cr oxide catalysts. *Bull. Chem. Soc. Jpn.* **1994**, *67*, 546–550. [[CrossRef](#)]
58. Pasupulety, N.; Driss, H.; Alhamed, Y.A.; Alzahrani, A.A.; Daous, M.A.; Petrova, L. Studies on Au/Cu-Zn-Al catalyst for methanol synthesis from CO₂. *Appl. Catal. A* **2015**, *504*, 308–318. [[CrossRef](#)]
59. Arena, F.; Barbera, K.; Italiano, G.; Bonura, G.; Spadaro, L.; Frusteri, F. Synthesis, characterization and activity pattern of Cu-ZnO/ZrO₂ catalysts in the hydrogenation of carbon dioxide to methanol. *J. Catal.* **2007**, *249*, 185–194. [[CrossRef](#)]
60. Arena, F.; Italiano, G.; Barbera, K.; Bordiga, S.; Bonura, G.; Spadaro, L.; Frusteri, F. Solid-state interactions, adsorption sites and functionality of Cu-ZnO/ZrO₂ catalysts in the CO₂ hydrogenation to CH₃OH. *Appl. Catal. A* **2008**, *350*, 16–23. [[CrossRef](#)]
61. Bonura, G.; Cordaro, M.; Cannilla, C.; Arena, F.; Frusteri, F. The changing nature of the active site of Cu-Zn-Zr catalysts for the CO₂ hydrogenation reaction to methanol. *Appl. Catal. B* **2014**, *152–153*, 152–161. [[CrossRef](#)]
62. Guo, X.; Mao, D.; Lu, G.; Wang, S.; Wu, G. Glycine-nitrate combustion synthesis of CuO-ZnO-ZrO₂ catalysts for methanol synthesis from CO₂ hydrogenation. *J. Catal.* **2010**, *271*, 178–185. [[CrossRef](#)]
63. Donphai, W.; Piriyaawate, N.; Witoon, T.; Jantaratana, P.; Varabuntoonvit, V.; Chareonpanich, M. Effect of magnetic field on CO₂ conversion over Cu-ZnO/ZrO₂ catalyst in hydrogenation reaction. *J. CO₂ Util.* **2016**, *16*, 204–211. [[CrossRef](#)]
64. Arena, F.; Italiano, G.; Barbera, K.; Bonura, G.; Spadaro, L.; Frusteri, F. Basic evidences for methanol-synthesis catalyst design. *Catal. Today* **2009**, *143*, 80–85. [[CrossRef](#)]
65. Gao, P.; Li, F.; Zhan, H.; Zhao, N.; Xiao, F.; Wei, W.; Zhong, L.; Wang, H.; Sun, Y. Influence of Zr on the performance of Cu/Zn/Al/Zr catalysts via hydrotalcite-like precursors for CO₂ hydrogenation to methanol. *J. Catal.* **2013**, *298*, 51–60. [[CrossRef](#)]

66. Yang, C.; Ma, Z.Y.; Zhao, N.; Wei, W.; Hu, T.D.; Sun, Y.H. Methanol synthesis from CO₂-rich syngas over a ZrO₂ doped CuZnO catalyst. *Catal. Today* **2006**, *115*, 222–227. [[CrossRef](#)]
67. Melián-Cabrera, I.; Granados, L.; Fierro, J.L.G. Pd-modified Cu–Zn catalysts for methanol synthesis from CO₂/H₂ mixtures: Catalytic structures and performance. *J. Catal.* **2002**, *210*, 285–294. [[CrossRef](#)]
68. Sahibzada, M. Pd-promoted Cu/ZnO catalyst systems for methanol synthesis from CO₂/H₂. *Chem. Eng. Res. Des.* **2000**, *78*, 943–946. [[CrossRef](#)]
69. Melian-Cabrera, O.; Granados, M.L.; Terreros, P.; Fierro, J.L.G. CO₂ hydrogenation over Pd-modified methanol synthesis catalysts. *Catal. Today* **1998**, *45*, 251–256. [[CrossRef](#)]
70. Ban, H.; Li, C.; Asami, K.; Fujimoto, K. Influence of rare-earth elements (La, Ce, Nd and Pr) on the performance of Cu/Zn/Zr catalyst for CH₃OH synthesis from CO₂. *Catal. Commun.* **2014**, *54*, 50–54. [[CrossRef](#)]
71. Guo, X.; Mao, D.; Lu, G.; Wang, S.; Wu, G. The influence of La doping on the catalytic behavior of Cu/ZrO₂ for methanol synthesis from CO₂ hydrogenation. *J. Mol. Catal. A* **2011**, *345*, 60–68. [[CrossRef](#)]
72. Batyrev, E.D.; van den Heuvel, J.C.; Beckers, J.; Jansen, W.P.A.; Castricum, H.L. The effect of the reduction temperature on the structure of Cu/ZnO/SiO₂ catalysts for methanol synthesis. *J. Catal.* **2005**, *229*, 136–143. [[CrossRef](#)]
73. Owen, G.; Hawkes, C.M.; Lloyd, D. Methanol synthesis from intermetallic precursors: Binary lanthanide-copper catalysts. *Appl. Catal.* **1987**, *33*, 405–430. [[CrossRef](#)]
74. Bonura, G.; Arena, F.; Mezzatesta, G.; Cannilla, C.; Spadaro, L.; Frusteri, F. Role of the ceria promoter and carrier on the functionality of Cu-based catalysts in the CO₂-to-methanol hydrogenation reaction. *Catal. Today* **2011**, *171*, 251–256. [[CrossRef](#)]
75. Li, M.; Zeng, Z.; Liao, F.; Hong, X.; Tsang, S.C.E. Enhanced CO₂ hydrogenation to methanol over CuZn nanoalloy in Ga modified Cu/ZnO catalysts. *J. Catal.* **2016**, *343*, 157–167. [[CrossRef](#)]
76. Toyir, J.; Ramírez de la Piscina, P.; Homs, N. Ga-promoted copper-based catalysts highly selective for methanol steam reforming to hydrogen; relation with the hydrogenation of CO₂ to methanol. *Int. J. Hydrogen Energy* **2015**, *40*, 11261–11266. [[CrossRef](#)]
77. Zhang, Y.; Li, D.; Zhang, Y.; Cao, Y.; Zhang, S.; Wang, K.; Ding, F.; Wu, J. V-modified CuO–ZnO–ZrO₂/HZSM-5 catalyst for efficient direct synthesis of DME from CO₂ hydrogenation. *Catal. Commun.* **2014**, *55*, 49–52. [[CrossRef](#)]
78. Zhang, Q.; Zuo, Y.-Z.; Han, M.-H.; Wang, J.-F.; Jin, Y.; Wei, F. Long carbon nanotubes intercrossed Cu/Zn/Al/Zr catalyst for CO/CO₂ hydrogenation to methanol/dimethyl ether. *Catal. Today* **2010**, *150*, 55–60. [[CrossRef](#)]
79. Deerattrakul, V.; Dittanet, P.; Sawangphruk, M.; Kongkachuichay, P. CO₂ hydrogenation to methanol using Cu-Zn catalyst supported on reduced graphene oxide nanosheets. *J. CO₂ Util.* **2016**, *16*, 104–113. [[CrossRef](#)]
80. Fan, Y.J.; Wu, S.F. A graphene-supported copper-based catalyst for the hydrogenation of carbon dioxide to form methanol. *J. CO₂ Util.* **2016**, *16*, 150–156. [[CrossRef](#)]
81. Ahmed, N.; Shibata, Y.; Taniguchi, T.; Izumi, Y. Photocatalytic conversion of carbon dioxide into methanol using zinc–copper–M (III)(M = aluminum, gallium) layered double hydroxides. *J. Catal.* **2011**, *279*, 123–135. [[CrossRef](#)]
82. Wang, G.; Zuo, Y.; Han, M.; Wang, J. Copper crystallite size and methanol synthesis catalytic property of Cu-based catalysts promoted by Al, Zr and Mn. *React. Kinet. Mech. Catal.* **2010**, *101*, 443–454. [[CrossRef](#)]
83. Ladera, R.; Pérez-Alonso, F.J.; González-Carballo, J.M.; Ojeda, M.; Rojas, S.; Fierro, J.L.G. Catalytic valorization of CO₂ via methanol synthesis with Ga-promoted Cu–ZnO–ZrO₂ catalysts. *Appl. Catal. B* **2013**, *142–143*, 241–248. [[CrossRef](#)]
84. Zhan, H.; Li, F.; Xin, C.; Zhao, N.; Xiao, F.; Wei, W.; Sun, Y. Performance of the La–Mn–Zn–Cu–O Based Perovskite Precursors for Methanol Synthesis from CO₂ Hydrogenation. *Catal. Lett.* **2015**, *145*, 1177–1185. [[CrossRef](#)]
85. Azizi, Z.; Rezaeimanesh, M.; Tohidian, T.; Rahimpour, M.R. Dimethyl ether: A review of technologies and production challenges. *Chem. Eng. Process.* **2014**, *82*, 150–172. [[CrossRef](#)]
86. Tavan, Y.; Hosseini, S.H.; Ghavipour, M.; Nikou, M.R.K.; Shariati, A. From laboratory experiments to simulation studies of methanol dehydration to produce dimethyl ether—Part I: Reaction kinetic study. *Chem. Eng. Process.* **2013**, *73*, 144–150. [[CrossRef](#)]

87. Khaleel, A. Titanium-doped alumina for catalytic dehydration of methanol to dimethyl ether at relatively low temperatures. *Fuel* **2011**, *90*, 2422–2427. [[CrossRef](#)]
88. Liu, D.; Yao, C.; Zhang, J.; Fan, D.; Chen, D. Catalytic dehydration of methanol to dimethyl ether over modified γ -Al₂O₃ catalyst. *Fuel* **2011**, *90*, 1738–1742. [[CrossRef](#)]
89. Mollavalli, M.; Yaripour, F.; Mohammadi-Jam, S.; Atashi, H. Relationship between surface acidity and activity of solid-acid catalysts in vapour phase dehydration of methanol. *Fuel Process. Technol.* **2009**, *90*, 1093–1098. [[CrossRef](#)]
90. Xia, J.; Mao, D.; Zhang, B.; Chen, Q.; Zhang, Y.; Tang, Y. Catalytic properties of fluorinated alumina for the production of dimethyl ether. *Catal. Commun.* **2006**, *7*, 362–366. [[CrossRef](#)]
91. Yaripour, F.; Shariatnia, Z.; Sahebdehfar, S.; Irandoukht, A. The effects of synthesis operation conditions on the properties of modified γ -alumina nanocatalysts in methanol dehydration to dimethyl ether using factorial experimental design. *Fuel* **2015**, *139*, 40–50. [[CrossRef](#)]
92. Xu, M.; Lunsford, J.H.; Goodman, D.W.; Bhattacharyya, A. Synthesis of dimethyl ether (DME) from methanol over solid-acid catalysts. *Appl. Catal. A* **1997**, *149*, 289–301. [[CrossRef](#)]
93. Yaripour, F.; Baghaei, F.; Schmidt, I.; Perregaard, J. Catalytic dehydration of methanol to dimethyl ether (DME) over solid-acid catalysts. *Catal. Commun.* **2005**, *6*, 147–152. [[CrossRef](#)]
94. Jun, K.W.; Lee, H.S.; Roh, H.S.; Park, S.E. Highly water-enhanced H-ZSM-5 catalysts for dehydration of methanol to dimethyl ether. *Bull. Korean Chem. Soc.* **2003**, *24*, 106–108.
95. Tao, J.; Jun, K.; Lee, K. Co-production of dimethyl ether and methanol from CO₂ hydrogenation: Development of a stable hybrid catalyst. *Appl. Organomet. Chem.* **2001**, *15*, 105–108. [[CrossRef](#)]
96. Alharbi, W.; Kozhevnikova, E.F.; Kozhevnikov, I.V. Dehydration of methanol to dimethyl ether over heteropoly acid catalysts: The relationship between reaction rate and catalyst acid strength. *ACS Catal.* **2015**, *5*, 7186–7193. [[CrossRef](#)]
97. Ladera, R.M.; Fierro, J.L.G.; Ojeda, M.; Rojas, S. TiO₂-supported heteropoly acids for low-temperature synthesis of dimethyl ether from methanol. *J. Catal.* **2014**, *312*, 195–203. [[CrossRef](#)]
98. Spivey, J. Review: Dehydration catalysts for the methanol/dimethyl ether reaction. *Chem. Eng. Commun.* **1991**, *110*, 123–142. [[CrossRef](#)]
99. Ciftci, A.; Sezgi, N.A.; Dogu, T. Nafion-incorporated silicate structured nanocomposite mesoporous catalysts for dimethyl ether synthesis. *Ind. Eng. Chem. Res.* **2010**, *49*, 6753–6762. [[CrossRef](#)]
100. Varisli, D.; Dogu, T. Production of clean transportation fuel dimethylether by dehydration of methanol over nafion catalyst. *Gazi Univ. J. Sci.* **2008**, *21*, 37–41.
101. Hosseinejad, S.; Afacan, A.; Hayes, R.E. Catalytic and kinetic study of methanol dehydration to dimethyl ether. *Chem. Eng. Res. Des.* **2012**, *90*, 825–833. [[CrossRef](#)]
102. Harmer, M.A.; Sun, Q. Solid acid catalysis using ion-exchange resins. *Appl. Catal. A* **2001**, *221*, 45–62. [[CrossRef](#)]
103. Frontera, P.; Macario, A.; Aloise, A.; Crea, F.; Antonucci, P.L.; Nagy, J.B.; Frusteri, F.; Giordano, G. Catalytic dry-reforming on Ni-zeolite supported catalyst. *Catal. Today* **2012**, *179*, 52–60. [[CrossRef](#)]
104. Frontera, P.; Macario, A.; Aloise, A.; Antonucci, P.L.; Giordano, G.; Nagy, J.B. Effect of support surface on methane dry-reforming catalyst preparation. *Catal. Today* **2013**, *218*, 18–29. [[CrossRef](#)]
105. Frontera, P.; Aloise, A.; Macario, A.; Antonucci, P.L.; Crea, F.; Giordano, G.; Nagy, J.B. Bimetallic zeolite catalyst for CO₂ reforming of methane. *Top. Catal.* **2010**, *53*, 265–272. [[CrossRef](#)]
106. Macario, A.; Giordano, G. Catalytic conversion of renewable sources for biodiesel production: A comparison between biocatalysts and inorganic catalysts. *Catal. Lett.* **2013**, *143*, 159–168. [[CrossRef](#)]
107. Macario, A.; Verri, F.; Diaz, U.; Corma, A.; Giordano, G. Pure silica nanoparticles for liposome/lipase system encapsulation: Application in biodiesel production. *Catal. Today* **2013**, *204*, 148–155. [[CrossRef](#)]
108. Corma, A. State of the art and future challenges of zeolites as catalysts. *J. Catal.* **2003**, *216*, 298–312. [[CrossRef](#)]
109. Vishwanathan, V.; Jun, K.; Kim, J.; Roh, H. Vapour phase dehydration of crude methanol to dimethyl ether over Na-modified H-ZSM-5 catalysts. *Appl. Catal. A* **2005**, *276*, 251–255. [[CrossRef](#)]
110. Migliori, M.; Aloise, A.; Catizzone, E.; Giordano, G. Kinetic analysis of methanol to dimethyl ether reaction over H-MFI catalyst. *Ind. Eng. Chem. Res.* **2014**, *53*, 14885–14891. [[CrossRef](#)]
111. Andzelm, J.; Goving, N.; Fitzgerald, G.; Maiti, A. DFT study of methanol conversion to hydrocarbons in a zeolite catalyst. *Int. J. Quantum Chem.* **2003**, *91*, 467–473. [[CrossRef](#)]

112. Wang, W.; Seiler, M.; Hunger, M. Role of surface methoxy species in the conversion of methanol to dimethyl ether on acidic zeolites investigated by in situ stopped-flow MAS NMR spectroscopy. *J. Phys. Chem. B* **2001**, *105*, 12553–12558. [[CrossRef](#)]
113. Migliori, M.; Aloise, A.; Giordano, G. Methanol to dimethylether on H-MFI catalyst: The influence of the Si/Al ratio on kinetic parameters. *Catal. Today* **2014**, *227*, 138–143. [[CrossRef](#)]
114. Tajima, N.; Tsuneda, T.; Toyama, F.; Hirao, K. A new mechanism for the first carbon–carbon bond formation in the MTG process: A theoretical study. *J. Am. Chem. Soc.* **1998**, *120*, 8222–8229. [[CrossRef](#)]
115. Teketel, S.; Olsbye, U.; Lillerud, K.P.; Beato, P.; Svelle, S. Co-conversion of methanol and light alkenes over acidic zeolite catalyst H-ZSM-22: Simulated recycle of non-gasoline range products. *Appl. Catal. A* **2015**, *494*, 68–76. [[CrossRef](#)]
116. Li, J.; Wei, Z.; Chen, Y.; Jing, B.; He, Y.; Dong, M.; Jiao, H.; Li, X.; Qin, Z.; Wang, J.; Fan, W. A route to form initial hydrocarbon pool species in methanol conversion to olefins over zeolites. *J. Catal.* **2014**, *317*, 277–283. [[CrossRef](#)]
117. Qi, L.; Wei, Y.; Xu, L.; Liu, Z. Reaction behaviors and kinetics during induction period of methanol conversion on HZSM-5 zeolite. *ACS Catal.* **2015**, *5*, 3973–3982. [[CrossRef](#)]
118. Svelle, S.; Joensen, F.; Nerlov, J.; Olsbye, U.; Lillerud, K.P.; Kolboe, S.; Bjørgen, M. Conversion of methanol into hydrocarbons over zeolite H-ZSM-5: Ethene formation is mechanistically separated from the formation of higher alkenes. *J. Am. Chem. Soc.* **2006**, *128*, 14770–14771. [[CrossRef](#)] [[PubMed](#)]
119. Campelo, J.M.; Lafont, F.; Marinas, J.M.; Ojeda, M. Studies of catalyst deactivation in methanol conversion with high, medium and small pore silicoaluminophosphates. *Appl. Catal. A* **2000**, *192*, 85–96. [[CrossRef](#)]
120. Palumbo, L.; Bonino, F.; Beato, P.; Bjørgen, M.; Zecchina, A.; Bordiga, S. Conversion of methanol to hydrocarbons: Spectroscopic characterization of carbonaceous species formed over H-ZSM-5. *J. Phys. Chem. C* **2008**, *112*, 9710–9716. [[CrossRef](#)]
121. Chua, Y.T.; Stair, P.C. An ultraviolet Raman spectroscopic study of coke formation in methanol to hydrocarbons conversion over zeolite H-MFI. *J. Catal.* **2003**, *213*, 39–46. [[CrossRef](#)]
122. Mentzel, U.V.; Højholt, K.; Holm, M.S.; Fehrmann, R.; Beato, P. Conversion of methanol to hydrocarbons over conventional and mesoporous H-ZSM-5 and H-Ga-MFI: Major differences in deactivation behavior. *Appl. Catal. A* **2012**, *417–418*, 290–297. [[CrossRef](#)]
123. Nushyama, N.; Kawaguchi, M.; Hirota, Y.; Van Vu, D.; Egashira, Y.; Ueyama, K. Size control of SAPO-34 crystals and their catalyst lifetime in the methanol-to-olefin reaction. *Appl. Catal. A Gen.* **2009**, *362*, 193–199. [[CrossRef](#)]
124. Deimund, M.A.; Schmidt, J.E.; Davis, M.E. Effect of pore and cage size on the formation of aromatic intermediates during the methanol-to-olefins reaction. *Top. Catal.* **2015**, *58*, 416–423. [[CrossRef](#)]
125. Catizzone, E.; Aloise, A.; Migliori, M.; Giordano, G. From 1-D to 3-D zeolite structures: Performance assessment in catalysis of vapour-phase methanol dehydration to DME. *Microporous Mesoporous Mater.* **2017**, *243*, 102–111. [[CrossRef](#)]
126. Catizzone, E.; Aloise, A.; Migliori, M.; Giordano, G. Dimethyl ether synthesis via methanol dehydration: Effect of zeolite structure. *Appl. Catal. A* **2015**, *502*, 215–220. [[CrossRef](#)]
127. Khandan, N.; Kazemeini, M.; Aghaziarati, M. Determining an optimum catalyst for liquid-phase dehydration of methanol to dimethyl ether. *Appl. Catal. A* **2008**, *349*, 6–12. [[CrossRef](#)]
128. Tang, Q.; Xu, H.; Zheng, Y.; Wang, J.; Li, H.; Zhang, J. Catalytic dehydration of methanol to dimethyl ether over micro-mesoporous ZSM-5/MCM-41 composite molecular sieves. *Appl. Catal. A* **2012**, *413–414*, 36–42. [[CrossRef](#)]
129. Rutkowska, M.; Macina, D.; Piwowska, Z.; Gajewska, M.; Diaz, U.; Chmielarz, L. Hierarchically structured ZSM-5 obtained by optimized mesotemplate-free method as active catalyst for methanol to DME conversion. *Catal. Sci. Technol.* **2016**, *6*, 4849–4862. [[CrossRef](#)]
130. Baek, S.-C.; Lee, Y.-J.; Jun, K.-W.; Hong, S.B. Influence of catalytic functionalities of zeolites on product selectivities in methanol conversion. *Energy Fuels* **2009**, *23*, 593–598. [[CrossRef](#)]
131. Catizzone, E.; Aloise, A.; Migliori, M.; Giordano, G. The effect of FER zeolite acid sites in methanol-to-dimethyl-ether catalytic dehydration. *J. Energy Chem.* **2017**, *26*, 406–415. [[CrossRef](#)]
132. Kim, S.D.; Baek, S.C.; Lee, Y.; Jun, K.; Kim, M.J.; Yoo, I.S. Effect of γ -alumina content on catalytic performance of modified ZSM-5 for dehydration of crude methanol to dimethyl ether. *Appl. Catal. A* **2006**, *309*, 139–143. [[CrossRef](#)]

133. Hassanpour, S.; Yaripour, F.; Taghizadeh, M. Performance of modified H-ZSM-5 zeolite for dehydration of methanol to dimethyl ether. *Fuel Process. Technol.* **2010**, *91*, 1212–1221. [[CrossRef](#)]
134. Khandan, N.; Kazemeini, M.; Aghaziarati, M. Dehydration of methanol to dimethyl ether employing modified H-ZSM-5 catalysts. *Iran. J. Chem. Eng.* **2009**, *6*, 3–11.
135. Hassanpour, S.; Taghizadeh, M.; Yaripour, F. Preparation, characterization, and activity evaluation of H-ZSM-5 catalysts in vapor-phase methanol dehydration to dimethyl ether. *Ind. Eng. Chem. Res.* **2010**, *49*, 4063–4069. [[CrossRef](#)]
136. Amaroli, T.; Simon, L.J.; Digne, M.; Montanari, T.; Bevilacqua, M.; Valtchev, V.; Patarin, J.; Busca, G. Effect of crystal size and Si/Al ratio on the surface properties of H-ZSM-5 zeolites. *Appl. Catal. A* **2006**, *306*, 78–84. [[CrossRef](#)]
137. García-Trenco, A.; Martínez, A. Direct synthesis of DME from syngas on hybrid CuZnAl/ZSM-5 catalysts: New insights into the role of zeolite acidity. *Appl. Catal. A* **2012**, *411–412*, 170–179. [[CrossRef](#)]
138. Frusteri, F.; Cordaro, M.; Cannilla, C.; Bonura, G. Multifunctionality of Cu–ZnO–ZrO₂/H-ZSM5 catalysts for the one-step CO₂-to-DME hydrogenation reaction. *Appl. Catal. B* **2015**, *162*, 57–65. [[CrossRef](#)]
139. Wang, D.; Han, Y.; Tan, Y.; Tsubaki, N. Effect of H₂O on Cu-based catalyst in one-step slurry phase dimethyl ether synthesis. *Fuel Process. Technol.* **2009**, *90*, 446–451. [[CrossRef](#)]
140. Diban, N.; Urriaga, A.M.; Ortiz, I.; Ereña, J.; Bilbao, J.; Aguayo, A.T. Influence of the membrane properties on the catalytic production of dimethyl ether with in situ water removal for the successful capture of CO₂. *Chem. Eng. J.* **2013**, *234*, 140–148. [[CrossRef](#)]
141. Iliuta, I.; Larachi, F.; Fongarland, P. Dimethyl ether synthesis with in situ H₂O removal in fixed-bed membrane reactor: Model and simulations. *Ind. Eng. Chem. Res.* **2010**, *49*, 6870–6877. [[CrossRef](#)]
142. Haw, J.F.; Song, W.; Marcus, D.M.; Nicholas, J.B. The mechanism of methanol to hydrocarbon catalysis. *Acc. Chem. Res.* **2003**, *36*, 317–326. [[CrossRef](#)] [[PubMed](#)]
143. Stich, I.; Gale, J.D.; Terakura, K.; Payne, M.C. Role of the zeolitic environment in catalytic activation of methanol. *J. Am. Chem. Soc.* **1999**, *121*, 3292–3302. [[CrossRef](#)]
144. Ivanova, S.; Lebrun, C.; Vanhaecke, E.; Pham-Huu, C.; Louis, B. Influence of the zeolite synthesis route on its catalytic properties in the methanol to olefin reaction. *J. Catal.* **2009**, *265*, 1–7. [[CrossRef](#)]
145. Naik, S.P.; Ryu, T.; Bui, V.; Miller, J.D.; Drinnan, N.B.; Zmierzak, W. Synthesis of DME from CO₂/H₂ gas mixture. *Chem. Eng. J.* **2011**, *167*, 362–368. [[CrossRef](#)]
146. Zhao, Y.; Chen, J.; Zhang, J. Effects of ZrO₂ on the performance of CuO–ZnO–Al₂O₃/HZSM-5 catalyst for dimethyl ether synthesis from CO₂ hydrogenation. *J. Nat. Gas Chem.* **2007**, *16*, 389–392. [[CrossRef](#)]
147. Park, Y.; Baek, S.; Ihm, S. CO₂ hydrogenation over copper-based hybrid catalysts for the synthesis of oxygenates. *Fuel Chem. Div. Prepr.* **2002**, *47*, 293–294.
148. Ereña, J.; Garona, R.; Arandes, J.M.; Aguayo, A.T.; Bilbao, J. Effect of operating conditions on the synthesis of dimethyl ether over a CuO–ZnO–Al₂O₃/NaHZSM-5 bifunctional catalyst. *Catal. Today* **2005**, *107–108*, 467–473. [[CrossRef](#)]
149. Wang, S.; Mao, D.; Guo, X.; Wu, X.; Lu, G. Dimethyl ether synthesis via CO₂ hydrogenation over CuO–TiO₂–ZrO₂/HZSM-5 bifunctional catalysts. *Catal. Commun.* **2009**, *10*, 1367–1370. [[CrossRef](#)]
150. Gao, W.; Wang, H.; Wang, Y.; Guo, W.; Jia, M. Dimethyl ether synthesis from CO₂ hydrogenation on La-modified CuO–ZnO–Al₂O₃/HZSM-5 bifunctional catalysts. *J. Rare Earths* **2013**, *31*, 470–476. [[CrossRef](#)]
151. Qi, G.X.; Fei, J.H.; Zheng, X.M.; Hou, Z.Y. DME synthesis from carbon dioxide and hydrogen over Cu–Mo/HZSM-5. *Catal. Lett.* **2001**, *72*, 121–124. [[CrossRef](#)]
152. Sun, K.; Lu, W.; Wang, M.; Xu, X. Low-temperature synthesis of DME from CO₂/H₂ over Pd-modified CuO–ZnO–Al₂O₃–ZrO₂/HZSM-5 catalysts. *Catal. Commun.* **2004**, *5*, 367–370. [[CrossRef](#)]
153. Zha, F.; Tian, H.; Yan, J.; Chang, Y. Multi-walled carbon nanotubes as catalyst promoter for dimethyl ether synthesis from CO₂ hydrogenation. *Appl. Surf. Sci.* **2013**, *285*, 945–951. [[CrossRef](#)]
154. Bonura, G.; Cannilla, C.; Frusteri, L.; Mezzapica, A.; Frusteri, F. DME production by CO₂ hydrogenation: Key factors affecting the behaviour of CuZnZr/ferrierite catalysts. *Catal. Today* **2017**, *281*, 337–344. [[CrossRef](#)]
155. Ereña, J.; Garoña, R.; Arandes, J.M.; Aguayo, A.T.; Bilbao, J. Direct synthesis of dimethyl ether from (H²+CO) and (H²+CO₂) feeds. Effect of feed composition. *Int. J. Chem. React. Eng.* **2005**, *3*. [[CrossRef](#)]
156. Zha, F.; Ding, J.; Chang, Y.; Ding, J.; Wang, J.; Ma, J. Cu–Zn–Al Oxide Cores Packed by Metal-Doped Amorphous Silica–Alumina Membrane for Catalyzing the Hydrogenation of Carbon Dioxide to Dimethyl Ether. *Ind. Eng. Chem. Res.* **2012**, *51*, 345–352. [[CrossRef](#)]

157. Liu, R.; Qin, Z.; Ji, H.; Su, T. Synthesis of dimethyl ether from CO₂ and H₂ using a Cu–Fe–Zr/HZSM-5 catalyst system. *Ind. Eng. Chem. Res.* **2013**, *52*, 16648–16655. [CrossRef]
158. Frusteri, F.; Migliori, M.; Cannilla, C.; Frusteri, L.; Catizzone, E.; Aloise, A.; Giordano, G.; Bonura, G. Direct CO₂-to-DME hydrogenation reaction: New evidences of a superior behaviour of FER-based hybrid systems to obtain high DME yield. *J. CO₂ Util.* **2017**, *18*, 353–361. [CrossRef]
159. Allahyari, S.; Haghghi, M.; Ebadi, A.; Hosseinzadeh, S. Effect of irradiation power and time on ultrasound assisted co-precipitation of nanostructured CuO–ZnO–Al₂O₃ over HZSM-5 used for direct conversion of syngas to DME as a green fuel. *Energy Convers. Manag.* **2014**, *83*, 212–222. [CrossRef]
160. Bonura, G.; Frusteri, F.; Cannilla, C.; Drago Ferrante, G.; Aloise, A.; Catizzone, E.; Migliori, M.; Giordano, G. Catalytic features of CuZnZr-zeolite hybrid systems for the direct CO₂-to-DME hydrogenation reaction. *Catal. Today* **2016**, *277*, 48–54. [CrossRef]
161. Frusteri, F.; Bonura, G.; Cannilla, C.; Drago Ferrante, G.; Aloise, A.; Catizzone, E.; Migliori, M.; Giordano, G. Stepwise tuning of metal-oxide and acid sites of CuZnZr-MFI hybrid catalysts for the direct DME synthesis by CO₂ hydrogenation. *Appl. Catal. B* **2015**, *176*, 522–531. [CrossRef]
162. Bansode, A.; Urakawa, A. Towards full one-pass conversion of carbon dioxide to methanol and methanol-derived products. *J. Catal.* **2014**, *309*, 66–70. [CrossRef]
163. Bae, J.W.; Kang, S.-H.; Lee, Y.-J.; Jun, K.-W. Effect of precipitants during the preparation of Cu–ZnO–Al₂O₃/Zr-ferrierite catalyst on the DME synthesis from syngas. *J. Ind. Eng. Chem.* **2009**, *15*, 566–572. [CrossRef]
164. Yang, G.; Tsubaki, N.; Shamoto, J.; Yoneyama, Y.; Zhang, Y. Confinement effect and synergistic function of H-ZSM-5/Cu–ZnO–Al₂O₃ capsule catalyst for one-step controlled synthesis. *J. Am. Chem. Soc.* **2010**, *132*, 8129–8136. [CrossRef] [PubMed]
165. Yang, G.; Thongkam, M.; Vitidsant, T.; Yoneyama, Y.; Tan, Y.; Tsubaki, N. A double-shell capsule catalyst with core-shell-like structure for one-step exactly controlled synthesis of dimethyl ether from CO₂ containing syngas. *Catal. Today* **2011**, *171*, 229–235. [CrossRef]
166. Nie, R.; Lei, H.; Pan, S.; Wang, L.; Fei, J.; Hou, Z. Core-shell structured CuO–ZnO@H-ZSM-5 catalysts for CO hydrogenation to dimethyl ether. *Fuel* **2012**, *96*, 419–425. [CrossRef]
167. Sun, K.; Lu, W.; Qiu, F.; Liu, S.; Xu, X. Direct synthesis of DME over bifunctional catalyst: Surface properties and catalytic performance. *Appl. Catal. A* **2003**, *252*, 243–249. [CrossRef]
168. García-Trenco, A.; Vidal-Moya, A.; Martínez, A. Study of the interaction between components in hybrid CuZnAl/HZSM-5 catalysts and its impact in the syngas-to-DME reaction. *Catal. Today* **2012**, *179*, 43–51. [CrossRef]
169. Jin, D.; Zhu, B.; Hou, Z.; Fei, J.; Lou, H.; Zheng, X. Dimethyl ether synthesis via methanol and syngas over rare earth metals modified zeolite Y and dual Cu–Mn–Zn catalysts. *Fuel* **2007**, *86*, 2707–2713. [CrossRef]
170. Stiefel, M.; Ahmad, R.; Arnold, U.; Döring, M. Direct synthesis of dimethyl ether from carbon-monoxide-rich synthesis gas: Influence of dehydration catalysts and operating conditions. *Fuel Process. Technol.* **2011**, *92*, 1466–1474. [CrossRef]
171. Chen, H.-J.; Fan, C.-W.; Yu, C.-S. Analysis, synthesis, and design of a one-step dimethyl ether production via a thermodynamic approach. *Appl. Energy* **2013**, *101*, 449–456. [CrossRef]
172. Moradi, G.R.; Yaripour, F.; Vale-Sheyda, P. Catalytic dehydration of methanol to dimethyl ether over mordenite catalysts. *Fuel Process. Technol.* **2010**, *91*, 461–468. [CrossRef]
173. Chen, W.-H.; Lin, B.-J.; Lee, H.-M.; Huang, M.-H. One-step synthesis of dimethyl ether from the gas mixture containing CO₂ with high space velocity. *Appl. Energy* **2012**, *98*, 92–101. [CrossRef]
174. Rownaghi, A.; Rezaei, F.; Stante, M.; Hedlund, J. Selective dehydration of methanol to dimethyl ether on ZSM-5 nanocrystals. *Appl. Catal. B* **2012**, *119*, 56–61. [CrossRef]
175. Raoof, F.; Taghizadeh, M.; Eliassi, A.; Yaripour, F. Effects of temperature and feed composition on catalytic dehydration of methanol to dimethyl ether over γ -alumina. *Fuel* **2008**, *87*, 2967–2971. [CrossRef]

